Interaction between the immune system and acute myeloid leukemia: A model incorporating promotion of regulatory T cell expansion by leukemic cells

Interaction Between the Immune System and Acute Myeloid Leukemia: A Model Incorporating Promotion of Regulatory T Cell Expansion by Leukemic Cells

Yoshiaki Nishiyama1, Yutaka Saikawa2 and Nobuaki Nishiyama1,3*
1 Graduate School of Natural Science and Technology,
Kanazawa University, Kakuma, Ishikawa, 9201192, Japan
2 Department of Pediatrics, Kanazawa Medical University,
Uchinada, Ishikawa, 9200293, Japan
3 Institute of Liberal Arts and Science, Kanazawa University,
Kakuma, Ishikawa, 9201192, Japan
* Corresponding author

ABSTRACT

Population dynamics of regulatory T cells (Treg) are crucial for the underlying interplay between leukemic and immune cells in progression of acute myeloid leukemia (AML). The goal of this work is to elucidate the dynamics of a model that includes Treg, which can be qualitatively assessed by accumulating clinical findings on the impact of activated immune cell infusion after selective Treg depletion. We constructed an ordinary differential equation model to describe the dynamics of three components in AML: leukemic blast cells, mature regulatory T cells (Treg), and mature effective T cells (Teff), including cytotoxic T lymphocytes. The model includes promotion of Treg expansion by leukemic blast cells, leukemic stem cell and progenitor cell targeting by Teff, and Treg-mediated Teff suppression, and exhibits two coexisting, stable steady states, corresponding to high leukemic cell load at diagnosis or relapse, and to long-term complete remission. Our model is capable of explaining the clinical findings that the survival of patients with AML after allogeneic stem cell transplantation is influenced by the duration of complete remission, and that cut-off minimal residual disease thresholds associated with a 100% relapse rate are identified in AML.

Keywords: acute myeloid leukemia; computational model; regulatory T cells; bistability; immunotherapy

1. Introduction

Cancer progression occurs through the dynamical crosstalk between cancer cells and immune cells involved in both immunosurveillance and tumor-promoting inflammation. A better understanding of their co-evolutionary dynamics and the underlying mechanism is therefore critical for improved treatment outcomes. The leukemias represent unique models to assess the impact of

cancer on the host immune system as the cancer cells and immune cells originate from the same hematopoietic tissue and are in close proximity in peripheral blood and bone marrow. The initial treatment for acute myeloid leukemia (AML) is intensive induction chemotherapy, which aims to diminish leukemic cells and restore normal hematopoiesis, leading to complete remission (CR). Even though many patients achieve CR with induction and consolidation chemotherapy, the relapse rate is still high. Early or higher recovery of peripheral blood lymphocytes, neutrophils or platelets after cytotoxic chemotherapy are favorable prognostic factors for survival in patients with AML [1,2], suggesting the essential role of bone marrow reconstitution and recovered or enhanced anti-leukemic activity in the inherent immune system.

On the other hand, the regulatory T cell (Treg) is a contributing factor to suppression of anti-leukemic activity [3]. While Tregs play a critical physiological role in immune tolerance to suppress excessive responses in allergy or autoimmunity [4,5] and to protect hematopoietic stem cells in bone marrow during inflammation [6], the immunosuppressive function of Tregs contributes to leukemia progression [6]. This has been supported by a growing body of evidence, which shows that lower frequency of Tregs at diagnosis is correlated with a higher rate of achieving CR [7], and that the frequency of Tregs in relapsed patients is dramatically higher [7], and that a high frequency of Tregs persists during CR [8-10].

A number of mechanistic mathematical models [11-16] have been proposed to explain cell population dynamics and the effects of chemotherapy and targeted therapy against leukemia, and have been calibrated against time evolution data for leukemia obtained from patients. Some studies of mathematical modeling have focused on the impact of immune responses on leukemia progression during chemotherapy [17-19]. In this work, we constructed an ordinary differential equation model to describe the dynamics of three components in AML: leukemic blast cells (L), mature regulatory T cells (Treg), and mature effective T cells (Teff), including cytotoxic T lymphocytes (CTLs). Our modeling strategy arises from the assumption of dynamic equilibrium among leukemic cells and blood cells, even in relapsed AML, leading to the system having two discrete, alternative stable steady states, one corresponding to leukemic cell dominance and the other to negligible leukemic cell load. Experimental evidence for bistability has been provided in diverse biological systems, and positive-feedback loops or mutually inhibitory, double negative-feedback loops have been proposed as the underlying mechanisms [20-24]. With a given parameter set, our model exhibits two coexisting, stable steady states corresponding to high leukemic cell load at diagnosis or relapse, and to long-term complete remission, and the transition between two steady states during chemotherapy and immunotherapy is simulated and visualized by trajectories over time in three-dimensional (variable) space. Such viewpoints are based on a dynamical systems framework for resilience [25].

In this work, we have interpreted the transient dynamics of the system spending time before

returning to the state of high leukemic cell load as corresponding to transient CR before relapse. In addition, our mathematical model can explain the clinical findings that the survival of patients with AML after allogeneic stem cell transplantation is influenced by the duration of CR [26,27] and that cut-off minimal residual disease (MRD) thresholds associated with a 100% relapse rate are identified in AML [28].

2. Materials and Methods

2.1 The model

Our interest is in the dynamics that originate from the mechanism by which immune cells paradoxically contribute to leukemia progression. While a number of models have focused on cancer cells and cancer-specific cells such as CTLs, our motivation leads to the present model including Treg as the third player, which could be assessed by accumulating clinical findings on the impact of activated immune cell infusion with selective Treg depletion.

Mature T cells, including CTLs and Tregs, are generated as a result of terminal differentiation in the hematopoietic hierarchy, in which hematopoietic stem cells (HSCs) at the top proliferate to give rise to progenitor cell types maintaining self-renewal ability. Leukemic stem cells (LSCs) and poorly differentiated leukemic progenitor cells with highly proliferative capability produce leukemic blast cells with resistance to apoptosis, leading to blast cell accumulation in peripheral blood [6]. In our model as illustrated in Fig. 1, we consider the populations of leukemic blast cells (L), mature regulatory T cells (Treg), and mature effective T cells (Teff), including CTLs. We assume that the dynamics of each cell population (L, Treg, Teff) are due to constant influx and first order decay by apoptosis, in which constant influx rates are denoted by aL, aTreg, and aTeff, and decay rate constants are denoted by dL, dTreg, and dTeff. In the model, the production of L results from the differentiation of LSCs and progenitor cells, and the production of Treg and Teff results from the differentiation of HSCs and progenitor cells. Together, aL, aTreg and aTeff are related to constant influxes from stem cells and progenitor cells collectively regarded as upstream cells. In addition, three intercellular interactions are identified as follows, and are modeled as Hill functions with threshold constants (k1, k2, k3) specifying the strength of intercellular interactions and the Hill coefficient p.

1) Leukemic stem cell and progenitor cell targeting by CTLs: experimental evidence has suggested CTL-mediated elimination of LSCs in a situation with low levels of IFN-γ [29] and myeloid leukemic progenitor cell targeting by alloreactive CTLs [30], leading to aL modulation by [Teff].

2) Treg-mediated effector T cell suppression: inhibition of the proliferation and differentiation of effector T cells [31], and IL2-dependent inhibition of CTL differentiation [32] have been proposed as the mechanisms of Treg-mediated suppression of immune responses and hematopoiesis, leading to aTeff modulation by [Treg].

3) Promotion of Treg formation by leukemic blast cells: The expression of PD-L1, indoleamine 2,3-dioxygenase (IDO) and CD200, a type-1 transmembrane glycoprotein in leukemic blast cells, promotes formation of Tregs [3,33-35], leading to aTreg modulation by [L].

Since the model proposed here is to be primitively assessed by focusing on dynamics after hypothetical treatment, chemotherapy and immunotherapy were designed to shift the system from one point to another in three-variable space in a simple manner as follows. We assume that the concentrations of drugs are constant and the decay rate of each cell population (L, Treg, Teff) is proportional only to the cell population ([L], [Treg], [Teff]) during induction chemotherapy. The rate constants of decay due to apoptosis and drugs are accordingly combined together as dL, dTreg, and dTeff during chemotherapy. Hematopoietic cell transplantation (HCT) or CTL infusion and Treg targeting as immunotherapy was modeled by instantaneous increases and decreases in [Teff] and [Treg], respectively.

The above model is translated into the following ordinary differential equations.

$$\frac{d[L]}{dt} = a_L\left(\frac{k_1^p}{k_1^p + [T_{eff}]^p}\right) - d_L[L] \quad 1.1$$

$$\frac{d[T_{eff}]}{dt} = a_{T_eff}\left(\frac{k_2^p}{k_2^p + [T_{reg}]^p}\right) - d_{T_{eff}}[T_{eff}] \quad 1.2$$

$$\frac{d[T_{reg}]}{dt} = a_{T_{reg}}\left(\frac{[L]^p}{k_3^p + [L]^p}\right) - d_{T_{reg}}[T_{reg}] \quad 1.3$$

2.2 Parameter estimation and simulation

Some parameters in Eq. (1) were estimated using Bayesian inference via a Markov chain Monte Carlo (MCMC) technique with clinical data for lymphocyte recovery after induction chemotherapy, which is described in the Results section below. We implemented PROC MCMC in SAS v.9.4 (SAS Institute, Cary, NC). PROC MCMC solved the ordinary differential equation defined in PROC FCMP and we used the resulting solution in the construction of the likelihood function. In MCMC PROC, the unknown parameters were modeled using random effects to account for time-series variability as follows: exp(β+α) where β denotes the fixed-effects parameter and α denotes the random-effects parameter with an unknown covariance matrix. Normal priors were used for β with N(0,10). The MCMC simulations were run for 20000 iterations and the first 1000 were considered burnin and removed.

Steady states of the model were determined as the intersection of three nullclines (d[L]/dt = 0,

d[Teff]/dt = 0 and d[Treg]/dt = 0), which were numerically solved using the nleqslv R-package [36]. The ordinary differential equations in Eqs. 1.1, 1.2, and 1.3 were numerically solved using ODE solvers from MATLAB (Ver. 7.13; The Mathworks, Inc.).

3. Results

Using the MCMC technique, we parameterized the model using clinical data reported by Kanakry et al. [37]. They reported the kinetics of early lymphocyte recovery after intensive induction timed sequential therapy for AML and examined the immunophenotypic profile of the recovering lymphocytes. A median of 73% of the lymphocytes were CD3+ cells, which were composed of 16.7% CD3+CD4+ cells and 66.4% CD3+CD8+ cells. They reported that the median ratio of CD3+CD4+ cells to CD3+CD8+ cells was 2.7:1 and regulatory T cells characterized by CD3+CD4+ subpopulation expressing Foxp3 constituted 10.5% of CD3+CD4+ cells. We estimated cell numbers of regulatory T cells and CTLs characterized by CD3+CD8+ expression at each time point in the time course of lymphocyte recovery presented by Kanakry et al., with the assumption that the above immunophenotypic profile is not changed during early lymphocyte recovery after intensive chemotherapy.

Assuming that [L] is approximately to be a constant [L]ss during complete remission (CR) after intensive induction chemotherapy, the model to be calibrated is Equations 1.2 and 1.3 with [L]ss. While < 5% leukemic blast cells among the total population of nucleated cells in bone marrow is included in the criteria for CR in AML, there is no definitive criterion for the peripheral blast count at CR. According to the clinical observation that 0% to 5% peripheral blast cells at CR had no effect on relapse free survival (RFS) time [38], we selected 100/μL for [L]ss during CR with 1% peripheral blast cells and 10000/μL as normal counts of peripheral nucleated cells.

Estimated means and standard deviations of β for aTeff, aTreg, dTeff and dTreg by the MCMC method are 4.03±0.47, 5.29±1.08, -1.60±0.78 and -3.23±2.74, respectively. The time courses of [Teff] and [Treg] obtained by numerical integration of Equations 1.2 and 1.3 with aTeff=56.53, aTreg=198.2, dTeff=0.2 and dTreg=0.04 as exp(means) are shown in Fig. 2, together with counts of CD3+CD8+ cells (CTLs) and CD3+CD4+Foxp3+ cells (regulatory T cells) estimated from lymphocyte recovery after induction chemotherapy reported by Kanakry et al. [37].

Dependencies of the steady-state concentrations of L, Teff, and Treg on the parameter k2, k3 and p reveal two stable steady states corresponding to high and low concentrations accompanied by one unstable steady state with intermediate concentrations, as shown in Fig. 3. While keeping the parameters aTreg, aTeff, dTreg, and dTeff to estimated values by the MCMC method, we searched a wide range of the parameter space of aL, dL, k1 and found parameter ranges characterized by the existence of one or two stable steady states separated by an unstable fixed point. The values of k2, k3 and p were set within the parameter ranges of bistability. However, we cannot exclude the

existence of different dynamics, such as a limit cycle. The values of model parameters in the present study are listed in Table 1.

We assume that the two stable steady states correspond to the state (SShi) of high leukemic cell load at diagnosis or relapse and the state (SSlo) of low leukemic cell load at long-term complete remission. In our simulations, the transitions from SShi to SSlo or the return to original SShi, which are induced by hypothetical chemotherapy and immunotherapy, were visualized as dynamical trajectories in three-dimensional space defined by the concentrations of L, Teff, and Treg.

Fig. 4a shows the trajectories from SShi ([L], [Teff], [Treg] = 100000/μL, 0.00031/μL, 4955/μL, out of figure) for chemotherapy with different values of dL. The locations of the state produced by chemotherapy shift toward SSlo ([L], [Teff], [Treg] = 40/μL, 283/μL, 8/μL) with increasing dL and determine whether the system reaches SSlo or returns to the original SShi. It is found that there are two basins of attraction in which the trajectories converge to SSlo and back to the original SShi. It is noted that the returning trajectories close to the boundary are attractive towards SSlo, compared with repulsive trajectories far from the boundary. Fig. 4b shows time courses corresponding to the returning trajectories. This indicates that the system spends considerable time in the vicinity of the boundary before returning to SShi. In Fig. 5, the state points leading to SShi are denoted by dots and those leading to SSlo are not marked, suggesting two basins of attraction. The latter can be seen as a blank region. It is noted that larger dots from which the system spends longer before returning to SShi are distributed along the boundary. We propose that transient CR with longer duration could be interpreted as having such transient dynamics [39] before returning to SShi, which could be considered in the framework of the resilience of dynamical systems [25].

There has been considerable interest in targeting Treg-mediated suppression of anti-AML reactive T cells. Bachanova et al. focused on the impact of prior Treg depletion followed by anti-leukemic cell infusion [40]. Patients with refractory AML received Treg depletion with IL-2 diphtheria toxin (IL2DT), which can selectively deplete IL-2 receptor-expressing cells, including Tregs. We simulated the impact of prior Treg depletion followed by Teff infusion. Teff infusion and Treg targeting were modeled by instantaneous modulations of [Teff] and [Treg] after hypothetical chemotherapy. An example is shown in Fig. 6. The returning trajectory to SShi after chemotherapy split into two trajectories. One is due to decreases in [Treg] followed by increases in [Teff] leading to SSlo. Another is due to only increases in [Teff], leading to the original SShi. The difference is due to whether or not the system crosses the basin boundary.

4. Discussion

The present model comprising L, Teff, and Treg, including promotion of Treg production by

L, exhibits two coexisting, stable steady states (SShi and SSlo) with a given parameter set. Assuming that SShi and SSlo correspond to the state at diagnosis or relapse and the state of long-term complete remission, the effects of hypothetical chemotherapy and immunotherapy inducing the transition from SShi to SSlo and returning to SShi are visualized as trajectories in three-dimensional space defined by L, Teff, and Treg concentrations.

Our results demonstrate that there is, in three-dimensional space, a boundary between two basins of attraction of SShi and SSlo, and that effective treatments move the trajectory to the basin of attraction of SSlo. That is, given the existence of the boundary, the strategy of treatment design leads to how the trajectory from SShi is forced to exceed the boundary and reach the region in which all states begin their trajectories converging to SSlo. This viewpoint is in line with an ecological resilience perspective on cancer [41]. Some mathematical models of cancer and immune cells interplay exhibit multistable steady states and were used to investigate the effectiveness of state transitions between the basins of attraction by the combination of hypothetical immunotherapy with chemotherapy [42,43] or radiation therapy [44]. Our model, which incorporates positive feedback between regulatory T cells and leukemic cells, also shows bistability with two basins of attraction, which serve as a framework for assessing extensive studies of immunotherapy targeting regulatory T cells of immunosuppressive activity and design of combined immunotherapy with chemotherapy. The predictions that flow from the putative existence of the basin boundary are the effectiveness of Teff infusion/Treg depletion and the effect of the number of infused cells exceeding the boundary in three-dimensional space. These predictions remain to be evaluated by clinical studies of immunotherapy.

The existence of the boundary suggested by this work may be supported by the findings of clinical studies of minimal residual disease (MRD) monitoring in leukemia. During CR attained with induction chemotherapy and maintenance treatment, submicroscopic amounts of residual leukemic cells in peripheral blood and bone marrow could not be identified cytomorphologically but could be sensitively detected by multiparameter flow cytometry (MFC) and quantitative real-time polymerase chain reaction (RT-qCR) in MRD monitoring [45,46]. Liu Yin et al. reported that RUNX1-RUNX1T1 and CBFB-MYH11 fusion transcripts during CR in patients with core binding factor (CBF) positive AML were quantified by qPCR for bone marrow (BM) and peripheral blood (PB) samples [28]. They identified MRD thresholds predicting whether cytomorphologically-detectable hematologic relapse occurs: hematologic relapse was 100% in patients with more than 500 RUNX1-RUNX1T1 copies in BM and more than 100 copies in PB, compared with 7% in patients with fewer than 500 copies and 7% in patients with fewer than 100 copies respectively, and 100% in patients with more than 50 CBFB-MYH11 copies in BM and 97% in patients with more than 10 copies in PB, compared with 10% in patients with fewer than 50 copies in BM and 7% in patients with fewer than 10 copies in PB respectively [28]. Several studies also reported MRD thresholds as independent

prognostic factors for predicting relapse occurrence in AML [47-49]. The MRD threshold can therefore be explained from the existence of the boundary found in our model.

We propose that transient CR before relapse with longer duration corresponds to the case in which the system spends longer near the boundary before returning to SShi. This leads to the prediction that longer duration of CR achieved by induction and consolidation chemotherapy is a favorable factor for outcomes of the subsequent chemotherapy and HCT or infusion of purified effector cells at relapse, as lower-dose chemotherapy or lower load of effector cells is needed for the system located near the boundary to exceed it and converge to SSlo. Our prediction is in line with better outcomes achieved by chemotherapy [50,51] and HCT [52] for relapsing patients with longer duration of first CR. The distribution of CR duration could be simulated with a threshold defining CR and be translated to a relapse free survival (RFS) curve. The simulated RFS curves could be directly compared with clinical outcomes in treatments of AML, resulting in the validation of our model to predict the impact of chemotherapy and immunotherapy for AML.

Another aspect of the trajectory crossing near the boundary is the accompanying transient increase in Teff concentration as shown in Fig. 4a. This leads to the prediction that higher absolute lymphocyte count (ALC) recovery is observed during CR with longer duration and is associated with a survival advantage for patients, which may be supported by ALC being identified as an independent prognostic factor for survival [53].

With our viewpoint of transient CR corresponding to the trajectory returning to SShi in three-dimensional space, relapse occurs without a change of parameter sets, in which coexisting stable steady states (SShi and SSlo) appear as shown in Fig. 3. On the other hand, assuming that the change of parameter values in our model is due to gene mutations during disease progression, the alternative explanation for relapse is possible. If the value of k2 decreases beyond the point of the bifurcation in Fig. 3a, the system remaining at SSlo is forced to go to SShi.

In summary, the dynamics of this model qualitatively explain some clinical findings of AML. Our model, which is yet to be further assessed against clinical data, may provide valuable information for the future design of combined immunotherapy with chemotherapy in AML.

Acknowledgements

We thank Mr. Tony Atkinson for his critical reading and advice on the manuscript. We also thank the referees for their valuable suggestions.

References

[1] U.Y. Malkan, G.G. Ayse, I.E. Eliacik, S. Etgul, T. Aslan, et al., Rebound thrombocytosis following induction chemotherapy is an independent predictor of a good prognosis in acute myeloid leukemia patients attaining first complete remission, Acta Haematol. 134(2015)32-37.

[2] M. Yanada, G. Borthakur, G. Garcia-Manero, F. Ravandi, S. Faderl, S. Pierce, et al., Blood counts at time of complete remission provide additional independent prognostic information in acute myeloid leukemia, Leuk Res. 32(10)(2008)1505-1509.

[3] C. Ustun, J.S. Miller, D.H. Munn, D.J. Weisdorf, B.R. Blazar, Regulatory T cells in acute myelogenous leukemia: is it time for immunomodulation? Blood 118(19)(2011)5084-5095.

[4] S. Lindley, C.M. Dayan, A. Bishop, B.O. Roep, M. Peakman, T.I.M. Tree, Defective suppressor function in CD4(+)CD25(+) T-cells from patients with type 1 diabetes, Diabetes. 54(1)(2005)92–99.

[5] R.J. DiPaolo, C. Brinster, T.S. Davidson, J. Andersson, D. Glass, E.M. Shevach, Autoantigen-specific TGFβ-induced Foxp3+ regulatory T cells prevent autoimmunity by inhibiting dendritic cells from activating autoreactive T cells, J Immunol. 179(7)(2007)4685–4693.

[6] C. Riether, C.M. Schurch, A.F. Ochsenbein, Regulation of hematopoietic and leukemic stem cells by the immune system, Cell Death and Differ. 22(2015)187-198.

[7] Z. Shenghui, H. Yixiang, W.Jianbo, Y. Kang, B. Laixi, Z. Yan, X. Xi, Elevated frequencies of CD4+CD25+CD127lo regulatory T cells is associated to poor prognosis in patients with acute myeloid leukemia, Int. J. Cancer 129(6)(2011)1373-1381.

[8] M.J. Szczepanski, M. Szajnik, M. Czystowska, M. Mandapathil, L. Strauss, A. Welsh, et al., Increased frequency and suppression by regulatory T cells in patients with acute myelogenous leukemia, Clin. Cancer Res. 15(10)(2009)3325-3332.

[9] E. Ersvaer, K. Liseth, J. Skavland, B.T. Gjertsen, Ø. Bruserud, Intensive chemotherapy for acute myeloid leukemia differentially affects circulating TC1, TH1, TH17 and TREG cells, BMC Immunol. 11(38)(2010).

[10] W. Yang, Y. Xu Clinical significance of Treg cell frequency in acute myeloid leukemia, Int. J. Hematol. 98(5)(2013)558-562.

[11] M.C. Mackey, C. Ou, L. Pujo-Menjouet, J. Wu, Periodic oscillations of blood cell populations in chronic myelogenous leukemia, SIAM J. Math. Anal. 38(1)(2006)166-187.

[12] D. Wodarz, N. Garg, N.L. Komarova, O. Benjamini, M.J. Keating, W.G. Wierda, et al., Kinetics of CLL cells in tissues and blood during therapy with the BTK inhibitor ibrutinib, Blood 123(26)(2014)4132-4135.

[13] F. Michor, T.P. Hughes, Y. Iwasa, S. Branford, N.P. Shah, C.L. Sawyers, M.A. Nowak,

Dynamics of chronic myeloid leukemia, Nature 435(7046)(2005)1267-1270.
[14] I. Roeder, M. Horn, I. Glauche, A. Hochhaus, M.C. Mueller, M. Loeffler, Dynamic modeling of imatinib-treated chronic myeloid leukemia: functional insights and clinical implications, Nature Med. 12(10)(2006)1181-1184.
[15] A.L. MacLean, S. Filippi, M.P. Stumpf, The ecology in the hematopoietic stem cell niche determines the clinical outcome in chronic myeloid leukemia, Proc. Natl. Acad. Sci. USA 111(10)(2014)3883-3888.
[16] T. Stiehl, N. Baran, A.D. Ho, A. Marciniak-Czochra, Cell division patterns in acute myeloid leukemia stem-like cells determine clinical course: a model to predict patient survival, Cancer Res. 75(6)(2015)940-949.
[17] V.A. Kuznetsov, I.A. Makalkin, M.A. Taylor, A.S. Perelson, Nonlinear dynamics of immunogenic tumors: parameter estimation and global bifurcation analysis, Bull. Math. Biol. 56(2)(1994)295–321.
[18] P.S. Kim, P.P. Lee, D. Levy, Dynamics and potential impact of the immune response to chronic myelogenous leukemia, PLoS Computational Biol. 4(6)(2008)e1000095.
[19] K. Roesch, D. Hasenclever, M. Scholz, Modelling lymphoma therapy and outcome, Bull. Math. Biol. 76(2)(2014)401-430.
[20] T.S. Gardner, C.R. Cantor, J.J. Collins, Construction of a genetic toggle switch in Escherichia coli, Nature 403(6767)(2000)339-342.
[21] D. Angeli, J.E. Ferrell, E.D. Sontag, Detection of multistability, bifurcations, and hysteresis in a large class of biological positive-feedback systems, Proc. Natl. Acad. Sci. USA 101(7)(2004)1822-1827.
[22] J.J. Tyson, R. Albert, A. Goldbeter, P. Ruoff, J. Sible, Biological switches and clocks, J. R. Soc. Interface 5(Suppl 1)(2008)S1–S8.
[23] J.E. Ferrell Jr., Bistability, bifurcation, and Waddington's epigenetic landscape, Curr. Biol. 22(11)(2012)R458-R466.
[24] L. Wanga, B.L. Walkera, S. Iannacconeb, D. Bhatta, P.J. Kennedya, W.T. Tse, Bistable switches control memory and plasticity in cellular differentiation, Proc. Natl. Sci. USA 106(16)(2009)6638-6643.
[25] K.Meyer, A mathematical review of resilience in ecology, Natural Resource Modeling, 29(3)(2016)339-352.
[26] E. Estey, Treatment of refractory AML, Leukemia 10(6)(1996)932-936.
[27] F.V. Michelis, E.G. Atenafu, V. Gupta, D.D. Kim, J. Kuruvilla, A. Lambie, et al., Duration of first remission, hematopoietic cell transplantation-specific comorbidity index and patient age predict survival of patients with AML transplanted in second CR, Bone Marrow Transplant. 48(11)(2013)1450-1455.

[28] J.A. Liu Yin, M.A. O'Brien, R.K. Hills, S.B. Daly, K. Wheatley, A.K. Burnett, Minimal residual disease monitoring by quantitative RT-PCR in core binding factor AML allows risk stratification and predicts relapse: results of the United Kingdom MRC AML-15 trial, Blood 120(2012)2826-2835.
[29] C. Schürch, C. Riether, M.A. Amrein, A.F. Ochsenbein, Cytotoxic T cells induce proliferation of chronic myeloid leukemia stem cells by secreting interferon-γ, J. Exp. Med. 210(2013)605-621.
[30] W.J. Norde, I.M. Overes, F. Maas, H. Fredrix, J.C. Vos, M.G. Kester, R. van der Voort, I. Jedema, J.H. Falkenburg, A.V. Schattenberg, T.M. de Witte, H. Dolstra, Myeloid leukemic progenitor cells can be specifically targeted by minor histocompatibility antigen LRH-1-reactive cytotoxic T cells, Blood 113(2009)2312-2323.
[31] S. Shen, Yi Ding, C.E. Tadokoro, D. Olivares-Villagómez, M. Camps-Ramírez, M.A.C. de Lafaille, J.J. Lafaille, Control of homeostatic proliferation by regulatory T cells, J. Clin. Invest. 115(2005)3517-3526.
[32] A. McNally, G.R. Hill, T. Sparwasser, R. Thomas, R.J. Steptoe, CD4+CD25+ regulatory T cells control CD8+ T-cell effector differentiation by modulating IL-2 homeostasis, Proc. Natl. Acad. Sci. USA 108(2011)7529-7534.
[33] A. Curti, S. Pandolfi, B. Valzasina, M. Aluigi, A. Isidori, E. Ferri, et al., Modulation of tryptophan catabolism by human leukemic cells results in the conversion of CD25- into CD25+ T regulatory cells, Blood 109(7)(2007)2871-2877.
[34] L.M. Francisco, V.H. Salinas, K.E. Brown, V.K. Vanguri, G.J. Freeman, V.K. Kuchroo, A.H. Sharpe, PD-L1 regulates the development, maintenance, and function of induced regulatory T cells, J. Exp. Med. 206(13)(2009)3015-3029.
[35] S.J. Coles, R.K. Hills, E.C. Wang, A.K. Burnett, S. Man, R.L. Darley, A.Tonks, Increased CD200 expression in acute myeloid leukemia is linked with an increased frequency of FoxP3+ regulatory T cells, Leukemia 26(9)(2012)2146-2148.
[36] B. Hasselman, nleqslv: Solving systems of non linear equations, R package version 2.1.1(2014).
[37] C.G. Kanakry, A.D. Hess, C.D.Gocke, C. Thoburn, F. Kos, C. Meyer, et al., Early lymphocyte recovery after intensive timed sequential chemotherapy for acute myelogenous leukemia: peripheral oligoclonal expansion of regulatory T cells, Blood 117(2)(2011)608-617.
[38] E.H.Estey, P.F.Thall, X.Wang, S.Verstovsek, J.Cortes, H.M.Kantarjian, Effect of circulating blasts at time of complete remission on subsequent relapse-free survival time in newly diagnosed AML, Blood 102(2003)3097-3099.
[39] J. Jaeger, D. Irons, N. Monk, The inheritance of process: a dynamical systems approach, J. Exp. Zool. B Mol. Dev. Evol. 318(8)(2012)591-612.
[40] V.Bachanova, S.Cooley, T.E.Defor, M.R.Verneris, B.Zhang, D.H.McKenna, J.Curtsinger, A.Panoskaltsis-Mortari, D.Lewis, K.Hippen, P.McGlave, D.J.Weisdorf, B.R.Blazar, J.S.Miller, Clearance of acute myeloid leukemia by haploidentical natural killer cells is improved using IL-2

diphtheria toxin fusion protein, Blood 123(25)(2014)3855-3863.
[41]A.C.Fassoni and H.M.Yang, An ecological resilience perspective on cancer: insights from a toy model, Ecological Complexity 30(2017)34-46.
[42] L.G. de Pillis, W. Gu, A.E. Radunskaya, Mixed immunotherapy and chemotherapy of tumors: modeling, applications and biological interpretations, Journal of theoretical Biology 238 (2006) 841-862.
[43] L.G. De Pillis, A. Radunskaya, A mathematical tumor model with immune resistance and drug therapy: an optimal control approach, Journal of Theoretical Medicine, 3(2001)841-862.
[44] M. Lu, B. Huanga, S.M. Hanash, J.N. Onuchica, E. Ben-Jacob, Modeling putative therapeutic implications of exosome exchange between tumor and immune cells, Proc. Natl. Acad. Sci. USA, 22(2014)E4165-E4174.
[45] W. Kern, C. Schoch, T. Haferlach, S. Schnittger, Monitoring of minimal residual disease in acute myeloid leukemia, Critical Reviews in Oncology/Hematology, 56 (2005) 283-309.
[46] S. Kayser, A. Benner, C. Thiede, U. Martens, J. Huber, P. Stadtherr, J.W.G. Janssen, C. Röllig, M.J. Uppenkamp, T. Bochtler, U. Hegenbart, G. Ehninger, A.D. Ho, P. Dreger, A. Krämer, Pretransplant NPM1 MRD levels predict outcome after allogeneic hematopoietic stem cell transplantation in patients with acute myeloid leukemia, Blood Cancer Journal 6(2016)e449.
[47] W. Zeijlemaker, A. Kelder, Y.J.M. Oussoren-Brockhoff, W.J. Scholten, A.N. Snel, D. Veldhuizen, J. Cloos, G.J. Ossenkoppele, G.J. Schuurhuis, Peripheral blood minimal residual disease may replace bone marrow minimal residual disease as an immunophenotypic biomarker for impending relapse in acute myeloid leukemia, Leukemia 30(2016)708-715.
[48] T. Kohnke, D. Sauter, K. Ringel, E. Hoster, R.P. Laubender, M. Hubmann, S.K. Bohlander, P.M. Kakadia, S. Schneider, A. Dufour, M.C. Sauerland, W.E. Berdel, T. Buchner, B. Wormann, J. Braess, W. Hiddemann, K. Spiekermann, M. Subklewe, Early assessment of minimal residual disease in AML by flow cytometry during aplasia identifies patients at increased risk of relapse, Leukemia 29(2015)377-386.
[49] V.H.J. van der Velden, A. van der Sluijs-Geling, B.E.S. Gibson, J.G. te Marvelde, P.G. Hoogeveen, W.C.J. Hop, K. Wheatley, M.B. Bierings, G.J. Schuurhuis, S.S.N. de Graaf, E.R. van Wering, J.J.M. van Dongen, Clinical significance of flowcytometric minimal residual disease detection in pediatric acute myeloid leukemia patients treated according to the DCOG ANLL97/MRC AML12 protocol, Leukemia 24(2010)1599-1606.
[50] W. Hiddemann, W.R. Martin, C.M. Sauerland, A. Heinecke, T.Büchner, Definition of refractoriness against conventional chemotherapy in acute myeloid leukemia: a proposal based on the results of retreatment by thioguanine, cytosine arabinoside, and daunorubicin (TAD 9) in 150 patients with relapse after standardized first line therapy, Leukemia 4(3)(1990)184-188.
[51] E.H. Estey, Treatment of relapsed and refractory acute myelogenous leukemia, Leukemia

14(3)(2000)476-479.
[52] F.V. Michelis, E.G. Atenafu, V. Gupta, D.D. Kim, J. Kuruvilla, A. Lambie, et al., Duration of first remission, hematopoietic cell transplantation-specific comorbidity index and patient age predict survival of patients with AML transplanted in second CR, Bone Marrow Transplant. 48(11)(2013)1450-1455.
[53] D. Behl, L.F. Porrata, S.N. Markovic, L. Letendre, R.K. Pruthi, C.C. Hook, et al., Absolute lymphocyte count recovery after induction chemotherapy predicts superior survival in acute myelogenous leukemia, Leukemia 20(1)(2006)29-34.

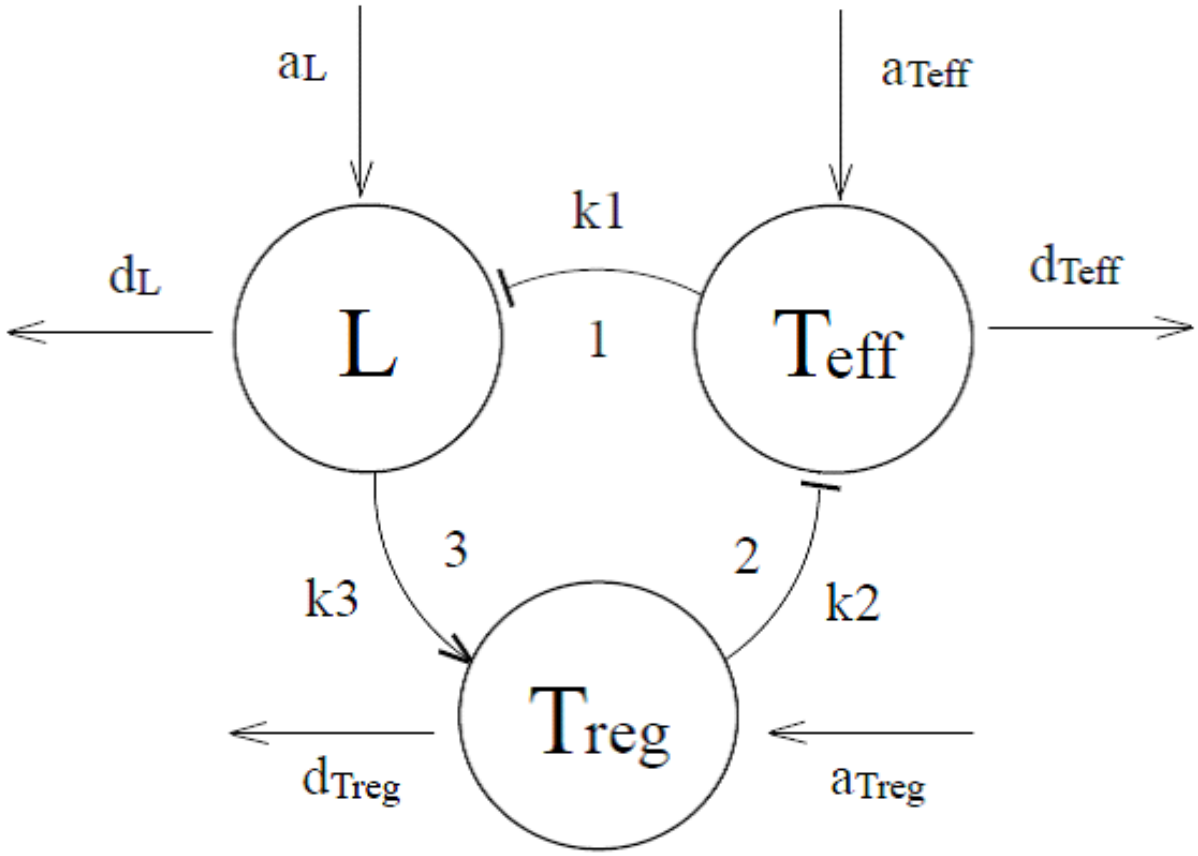

Fig. 1: Mechanistic model for crosstalk among leukemic cells and immune cells in AML. The processes of cell-cell interaction are numbered as follows: 1. Leukemic stem cells and progenitor cells targeted by effector T cells, 2. Effector T cell suppression mediated by Treg, and 3. Treg formation promoted by leukemic blast cells (L).

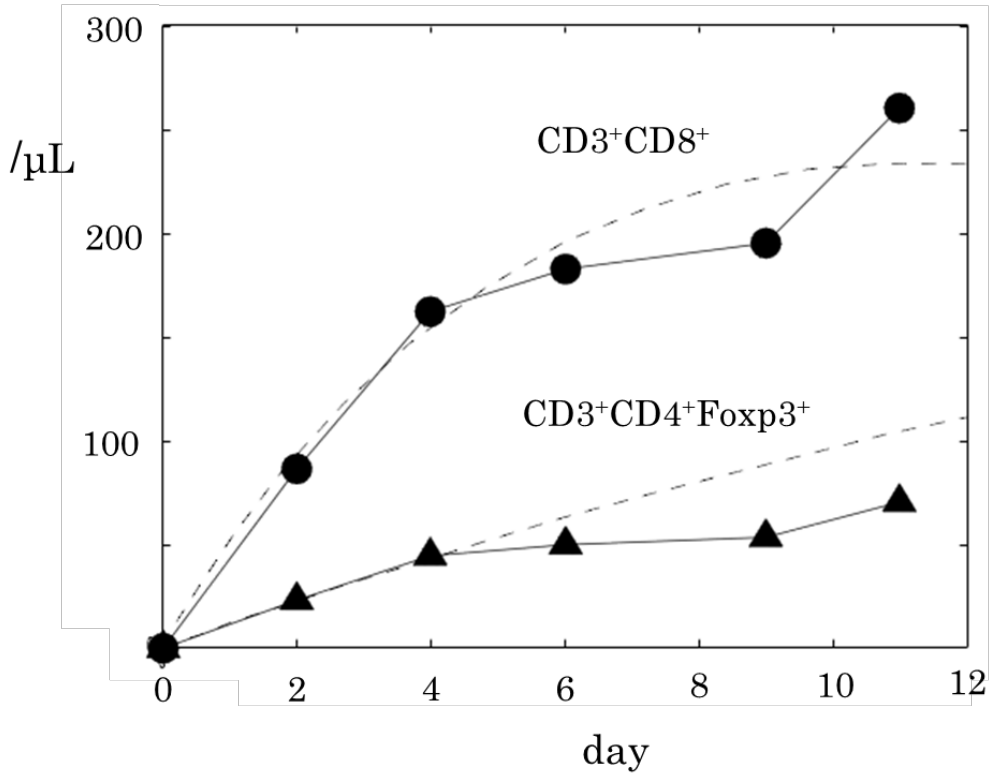

Fig. 2: Time courses of counts of CD3+CD8+ cells (CTLs, closed circles) and CD3+CD4+Foxp3+ cells (regulatory T cells, closed triangles) estimated from lymphocyte recovery after induction chemotherapy reported by Kanakry et al. [37]. Dashed lines show time courses of [Teff] and [Treg] obtained by numerical integration of Eqs 1.2 and 1.3 with aTeff=56.53, aTreg=198.2, dTeff=0.2 and dTreg=0.04 estimated by an MCMC technique.

Symbol	Value
cell influx	
a_L	0.1 - 1000 $\mu L^{-1} day^{-1}$
a_{Teff}	56.53 $\mu L^{-1} day^{-1}$
a_{Treg}	198.2 $\mu L^{-1} day^{-1}$
cell decay	
d_L	0.0001 - 1.0 day^{-1}
d_{Teff}	0.2 day^{-1}
d_{Treg}	0.04 day^{-1}
cell interaction	
k_1	1 - 1000 μL^{-1}
k_2	160 μL^{-1}
k_3	200 μL^{-1}
hill coefficient	
p	1-10

Table 1: Parameter Values Used in the Simulation

Fig. 3: Steady states as a function of the threshold constant k2 of a) leukemic blast cells (L), b) mature effective T cells (Teff), and c) mature regulatory T cells (Treg), and of the threshold constant k3 of d) leukemic blast cells (L), and of the Hill coefficient p of e) leukemic blast cells (L). Steady states along the solid lines are stable and steady states along dashed lines are unstable. Parameter ranges characterized by the existence of two stable steady states separated by an unstable fixed point are marked by gray backgrounds. Parameter values are aL=1000, aTeff=56.53, aTreg=198.2, dL=0.01, dTeff=0.2, dTreg=0.04, k1=40, k3=200, and p=4 for a), b), c) ,and aL=1000, aTeff=56.53, aTreg=198.2, dL=0.01, dTeff=0.2, dTreg=0.04, k1=40, k2=160, and p=4 for d), and aL=1000, aTeff=56.53, aTreg=198.2, dL=0.01, dTeff=0.2, dTreg=0.04, k1=40, k2=160, and k3=200 for e).

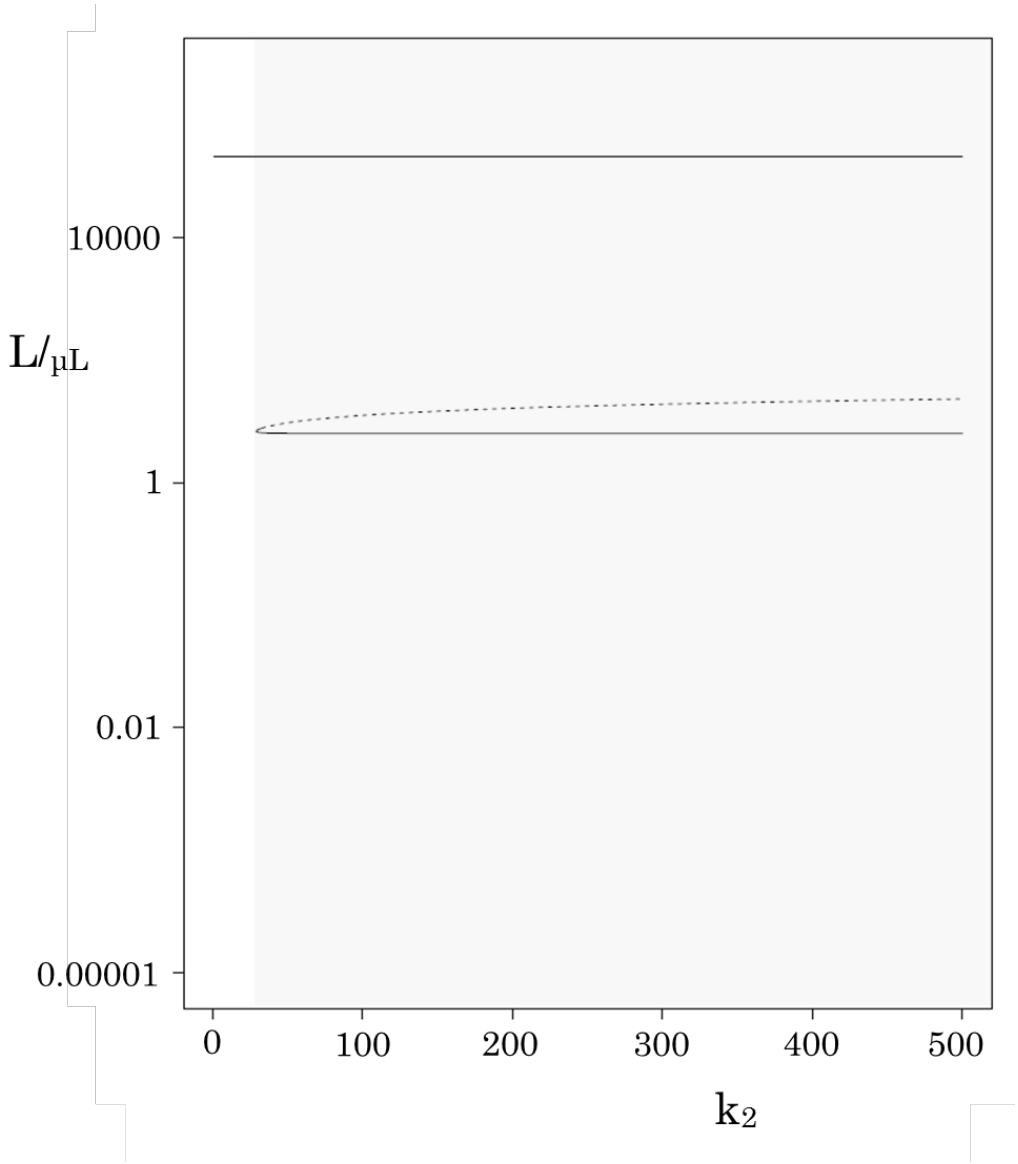

Fig. 3a

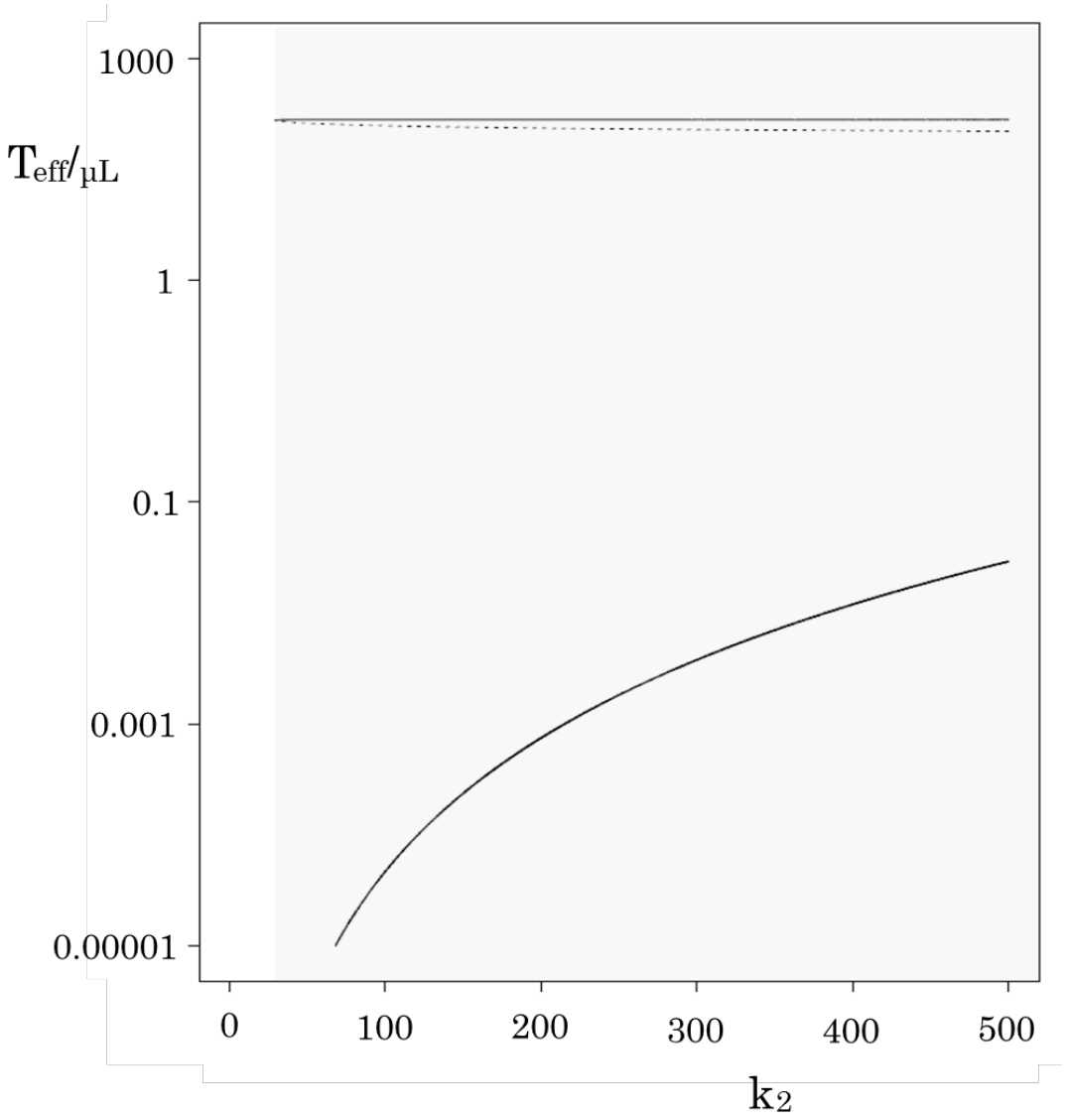

Fig. 3b

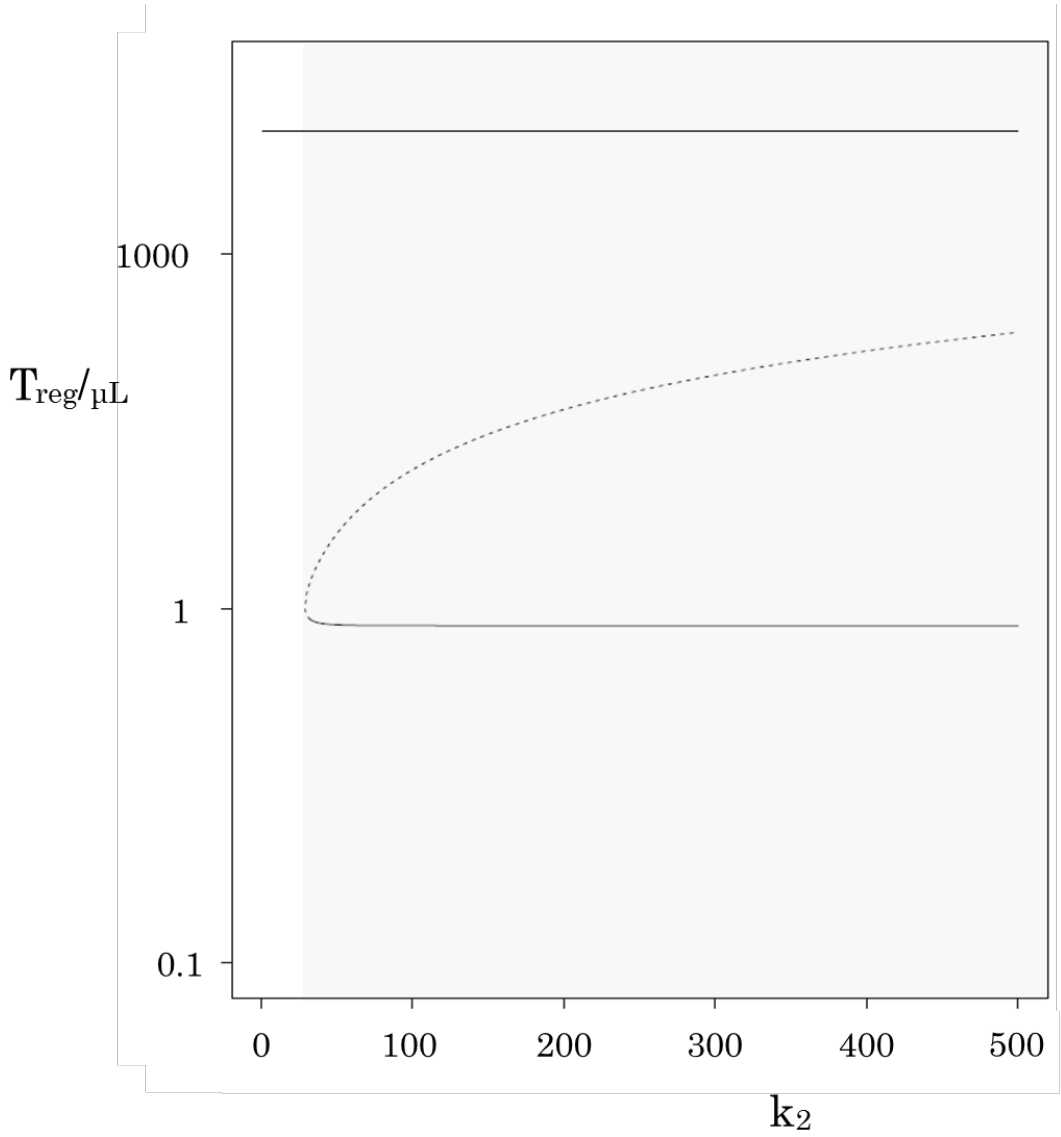

Fig. 3c

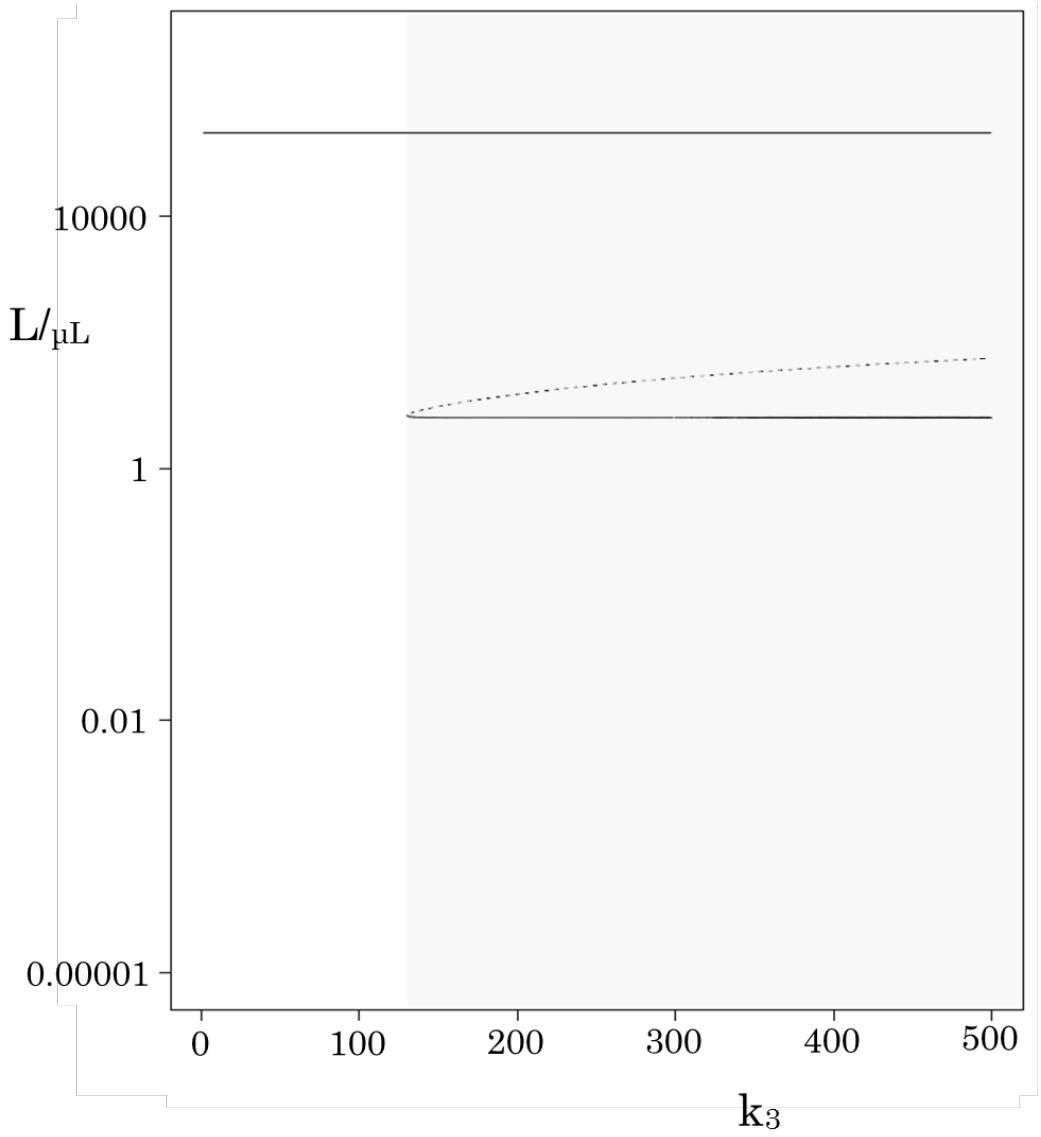

Fig.3d

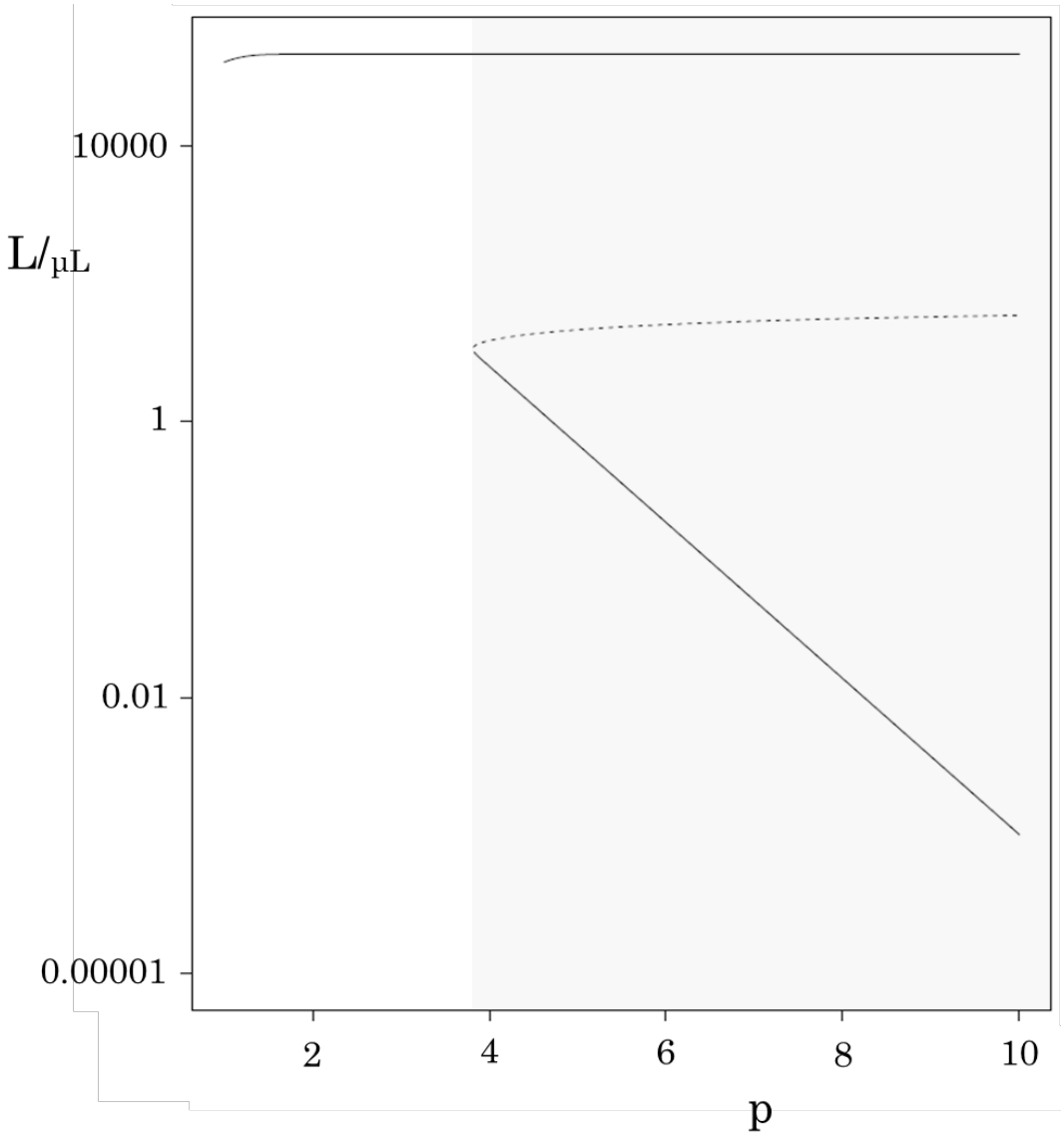

Fig. 3e

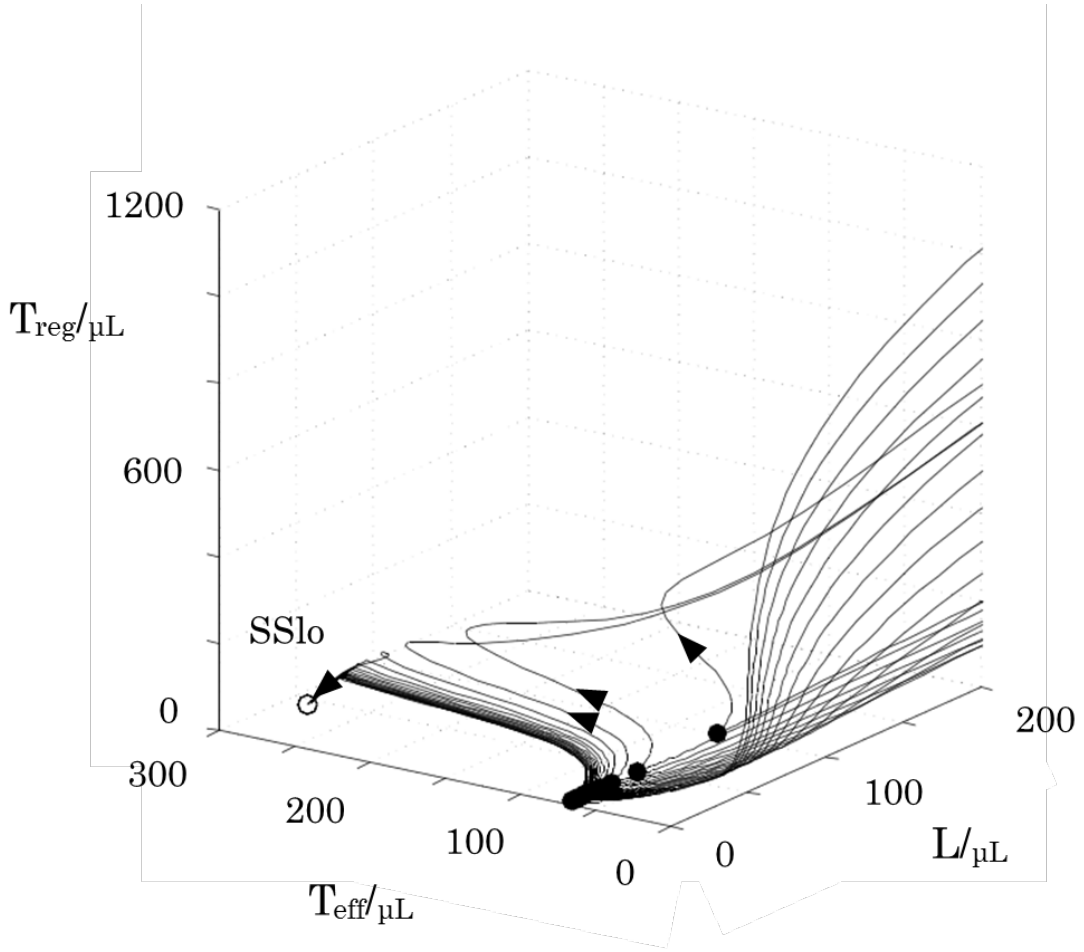

Fig. 4a: The trajectories from SShi (not shown in figure) after chemotherapy with different values of dL. The locations of the state produced by chemotherapy are denoted by closed circles. For higher dL, the trajectories with dL beyond a critical value change direction from returning to SShi to converging to SSlo, suggesting two basins of attraction. SShi ([L], [Teff], [Treg] = 100000/μL, 0.00031/μL, 4955/μL, out of figure) and SSlo ([L], [Teff], [Treg] = 40/μL, 283/μL, 8/μL, open circle in figure) were calculated with dL=0.01. Other parameter values are aL=1000, aTeff=56.53, aTreg=198.2, dTeff=0.2, dTreg=0.04, k1=40, k2=160, k3=200, and p=4. For a chemotherapy duration of 10 days, the decay rate constants were dTeff=0.8, dTreg=5.0, and dL was changed from 1.0 to 20.0.

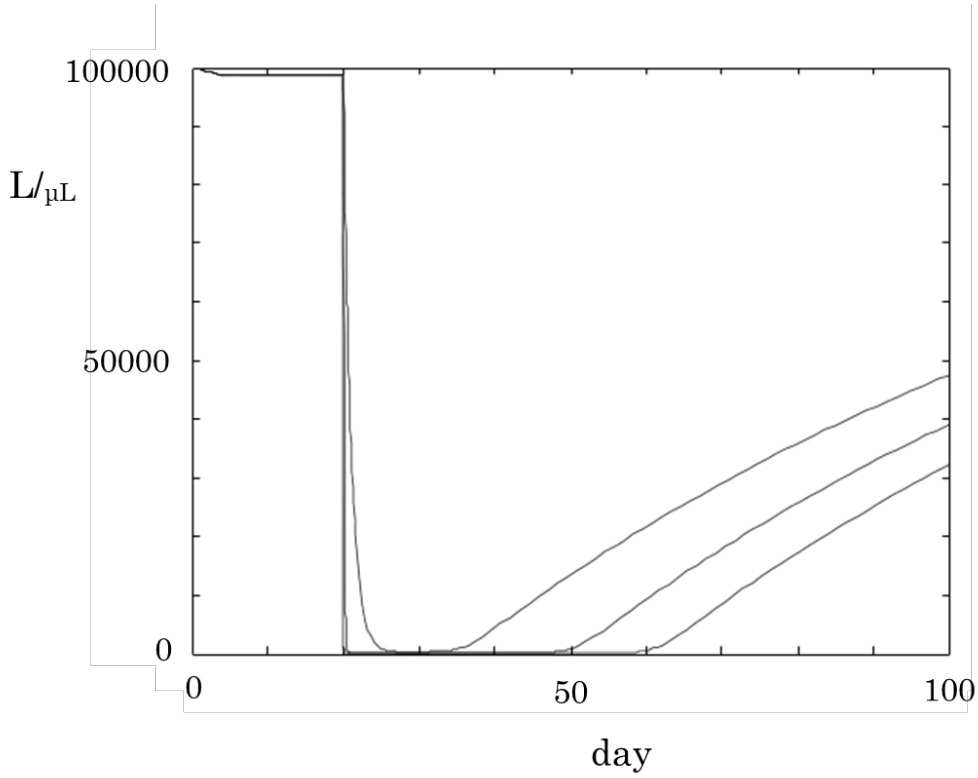

Fig. 4b: Time courses corresponding to the trajectories returning to SShi. The start of relapse is delayed with increasing dL. Parameter values are aL=1000, aTeff=56.53, aTreg=198.2, dL=0.01, dTeff=0.2, dTreg=0.04, k1=40, k2=160, k3=200, and p=4. For a chemotherapy duration of 10 days, the decay rate constants were dTeff=1.0, dTreg=5.0 and dL were 1.0, 10.0 and 100.0.

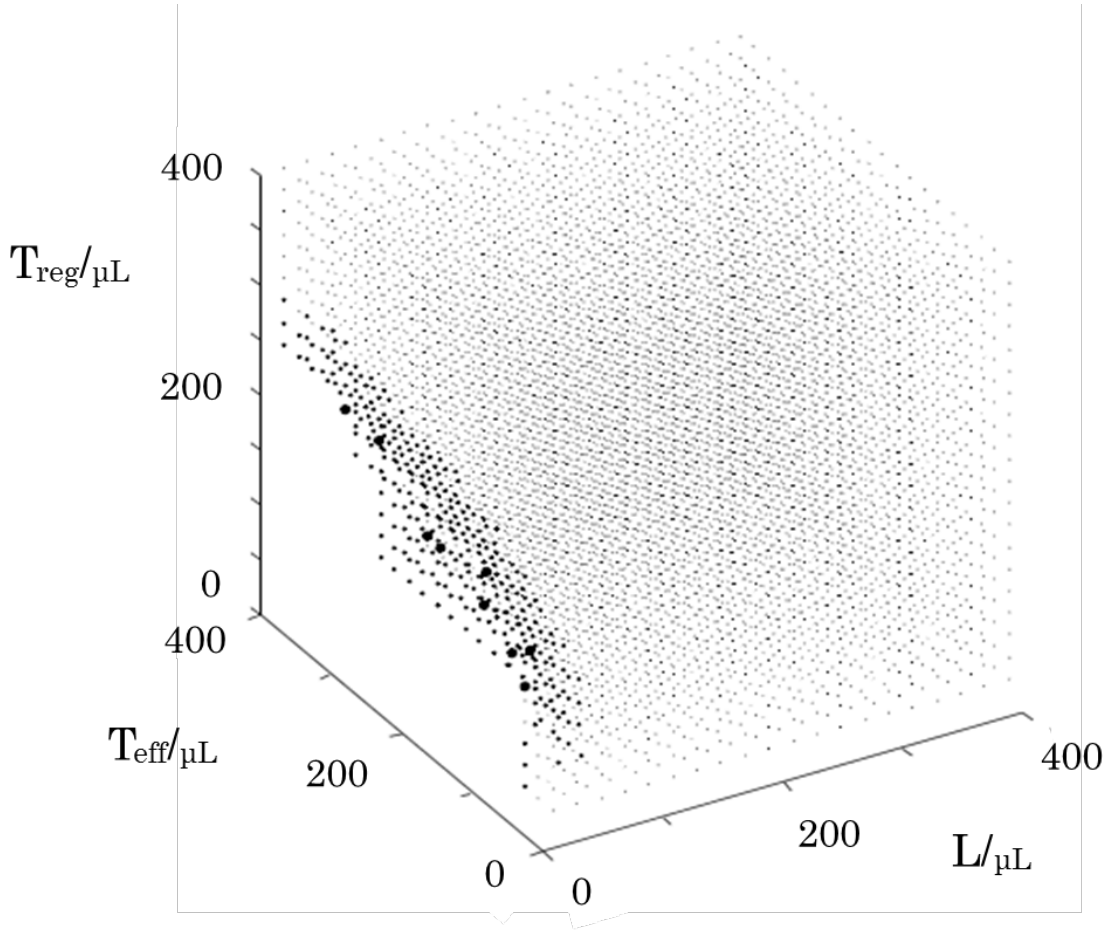

Fig. 5: The basin of attraction of SShi. The size of each dot in the basin indicates the time required for the system to arrive at SShi from the state denoted by a dot. It takes longer for the system to arrive at SShi from states distributed along the basin boundary. Parameter values are aL=1000, aTeff=56.53, aTreg=198.2, dL=0.01, dTeff=0.2, dTreg=0.04, k1=40, k2=160, k3=200, and p=4.

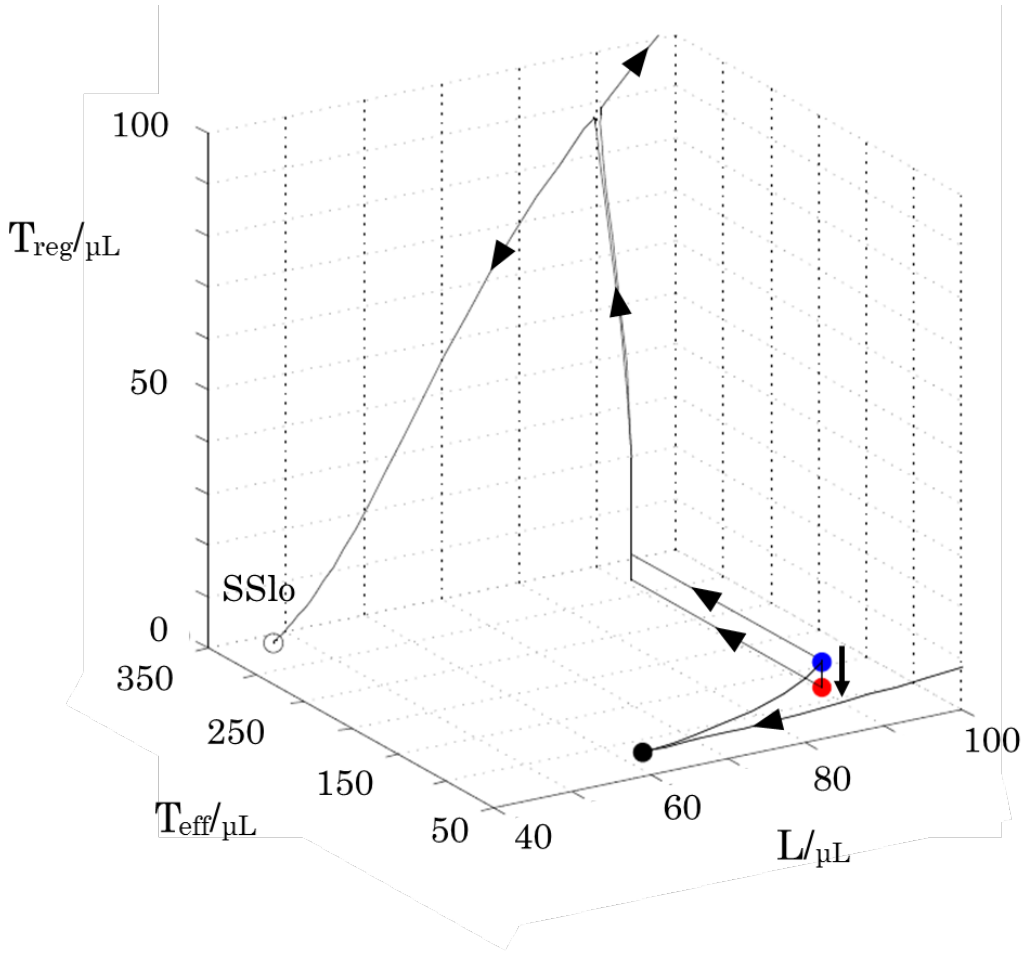

Fig. 6: Effects of Teff infusion only and prior Treg depletion followed by Teff infusion for the system on the trajectory returning to SShi in hypothetical immunotherapy. The instantaneous modulations ([Teff]+200/μl and [Treg]-5/μl) were applied at the point denoted by the blue circle. The Treg depletion forced the system from the point denoted by the blue circle to one denoted by the red circle. The same Teff infusions applied to the points denoted by blue and red circles result in two trajectories, one of which arrives at SSlo (open circle) and another returns to SShi (out of figure). Parameter values are aL=1000, aTeff=56.53, aTreg=198.2, dL=0.01, dTeff=0.2, dTreg=0.04, k1=40, k2=160, k3=200, and p=4. For a chemotherapy duration of 10 days, the decay rate constants were dL=1.0, dTeff=0.7, and dTreg=5.0.

Interaction Between the Immune System and Acute Myeloid Leukemia: A Model Incorporating Promotion of Regulatory T Cell Expansion by Leukemic Cells

Yoshiaki Nishiyama1, Yutaka Saikawa2 and Nobuaki Nishiyama1,3*
1 Graduate School of Natural Science and Technology,
Kanazawa University, Kakuma, Ishikawa, 9201192, Japan
2 Department of Pediatrics, Kanazawa Medical University,
Uchinada, Ishikawa, 9200293, Japan
3 Institute of Liberal Arts and Science, Kanazawa University,
Kakuma, Ishikawa, 9201192, Japan
* Corresponding author

ABSTRACT

Population dynamics of regulatory T cells (Treg) are crucial for the underlying interplay between leukemic and immune cells in progression of acute myeloid leukemia (AML). The goal of this work is to elucidate the dynamics of a model that includes Treg, which can be qualitatively assessed by accumulating clinical findings on the impact of activated immune cell infusion after selective Treg depletion. We constructed an ordinary differential equation model to describe the dynamics of three components in AML: leukemic blast cells, mature regulatory T cells (Treg), and mature effective T cells (Teff), including cytotoxic T lymphocytes. The model includes promotion of Treg expansion by leukemic blast cells, leukemic stem cell and progenitor cell targeting by Teff, and Treg-mediated Teff suppression, and exhibits two coexisting, stable steady states, corresponding to high leukemic cell load at diagnosis or relapse, and to long-term complete remission. Our model is capable of explaining the clinical findings that the survival of patients with AML after allogeneic stem cell transplantation is influenced by the duration of complete remission, and that cut-off minimal residual disease thresholds associated with a 100% relapse rate are identified in AML.

Keywords: acute myeloid leukemia; computational model; regulatory T cells; bistability; immunotherapy

1. Introduction

Cancer progression occurs through the dynamical crosstalk between cancer cells and immune cells involved in both immunosurveillance and tumor-promoting inflammation. A better understanding of their co-evolutionary dynamics and the underlying mechanism is therefore critical for improved treatment outcomes. The leukemias represent unique models to assess the impact of

cancer on the host immune system as the cancer cells and immune cells originate from the same hematopoietic tissue and are in close proximity in peripheral blood and bone marrow. The initial treatment for acute myeloid leukemia (AML) is intensive induction chemotherapy, which aims to diminish leukemic cells and restore normal hematopoiesis, leading to complete remission (CR). Even though many patients achieve CR with induction and consolidation chemotherapy, the relapse rate is still high. Early or higher recovery of peripheral blood lymphocytes, neutrophils or platelets after cytotoxic chemotherapy are favorable prognostic factors for survival in patients with AML [1,2], suggesting the essential role of bone marrow reconstitution and recovered or enhanced anti-leukemic activity in the inherent immune system.

On the other hand, the regulatory T cell (Treg) is a contributing factor to suppression of anti-leukemic activity [3]. While Tregs play a critical physiological role in immune tolerance to suppress excessive responses in allergy or autoimmunity [4,5] and to protect hematopoietic stem cells in bone marrow during inflammation [6], the immunosuppressive function of Tregs contributes to leukemia progression [6]. This has been supported by a growing body of evidence, which shows that lower frequency of Tregs at diagnosis is correlated with a higher rate of achieving CR [7], and that the frequency of Tregs in relapsed patients is dramatically higher [7], and that a high frequency of Tregs persists during CR [8-10].

A number of mechanistic mathematical models [11-16] have been proposed to explain cell population dynamics and the effects of chemotherapy and targeted therapy against leukemia, and have been calibrated against time evolution data for leukemia obtained from patients. Some studies of mathematical modeling have focused on the impact of immune responses on leukemia progression during chemotherapy [17-19]. In this work, we constructed an ordinary differential equation model to describe the dynamics of three components in AML: leukemic blast cells (L), mature regulatory T cells (Treg), and mature effective T cells (Teff), including cytotoxic T lymphocytes (CTLs). Our modeling strategy arises from the assumption of dynamic equilibrium among leukemic cells and blood cells, even in relapsed AML, leading to the system having two discrete, alternative stable steady states, one corresponding to leukemic cell dominance and the other to negligible leukemic cell load. Experimental evidence for bistability has been provided in diverse biological systems, and positive-feedback loops or mutually inhibitory, double negative-feedback loops have been proposed as the underlying mechanisms [20-24]. With a given parameter set, our model exhibits two coexisting, stable steady states corresponding to high leukemic cell load at diagnosis or relapse, and to long-term complete remission, and the transition between two steady states during chemotherapy and immunotherapy is simulated and visualized by trajectories over time in three-dimensional (variable) space. Such viewpoints are based on a dynamical systems framework for resilience [25].

In this work, we have interpreted the transient dynamics of the system spending time before

returning to the state of high leukemic cell load as corresponding to transient CR before relapse. In addition, our mathematical model can explain the clinical findings that the survival of patients with AML after allogeneic stem cell transplantation is influenced by the duration of CR [26,27] and that cut-off minimal residual disease (MRD) thresholds associated with a 100% relapse rate are identified in AML [28].

2. Materials and Methods

2.1 The model

Our interest is in the dynamics that originate from the mechanism by which immune cells paradoxically contribute to leukemia progression. While a number of models have focused on cancer cells and cancer-specific cells such as CTLs, our motivation leads to the present model including Treg as the third player, which could be assessed by accumulating clinical findings on the impact of activated immune cell infusion with selective Treg depletion.

Mature T cells, including CTLs and Tregs, are generated as a result of terminal differentiation in the hematopoietic hierarchy, in which hematopoietic stem cells (HSCs) at the top proliferate to give rise to progenitor cell types maintaining self-renewal ability. Leukemic stem cells (LSCs) and poorly differentiated leukemic progenitor cells with highly proliferative capability produce leukemic blast cells with resistance to apoptosis, leading to blast cell accumulation in peripheral blood [6]. In our model as illustrated in Fig. 1, we consider the populations of leukemic blast cells (L), mature regulatory T cells (Treg), and mature effective T cells (Teff), including CTLs. We assume that the dynamics of each cell population (L, Treg, Teff) are due to constant influx and first order decay by apoptosis, in which constant influx rates are denoted by aL, aTreg, and aTeff, and decay rate constants are denoted by dL, dTreg, and dTeff. In the model, the production of L results from the differentiation of LSCs and progenitor cells, and the production of Treg and Teff results from the differentiation of HSCs and progenitor cells. Together, aL, aTreg and aTeff are related to constant influxes from stem cells and progenitor cells collectively regarded as upstream cells. In addition, three intercellular interactions are identified as follows, and are modeled as Hill functions with threshold constants (k1, k2, k3) specifying the strength of intercellular interactions and the Hill coefficient p.

1) Leukemic stem cell and progenitor cell targeting by CTLs: experimental evidence has suggested CTL-mediated elimination of LSCs in a situation with low levels of IFN-γ [29] and myeloid leukemic progenitor cell targeting by alloreactive CTLs [30], leading to aL modulation by [Teff].

2) Treg-mediated effector T cell suppression: inhibition of the proliferation and differentiation of effector T cells [31], and IL2-dependent inhibition of CTL differentiation [32] have been proposed as the mechanisms of Treg-mediated suppression of immune responses and hematopoiesis, leading to aTeff modulation by [Treg].

3) Promotion of Treg formation by leukemic blast cells: The expression of PD-L1, indoleamine 2,3-dioxygenase (IDO) and CD200, a type-1 transmembrane glycoprotein in leukemic blast cells, promotes formation of Tregs [3,33-35], leading to aTreg modulation by [L].

Since the model proposed here is to be primitively assessed by focusing on dynamics after hypothetical treatment, chemotherapy and immunotherapy were designed to shift the system from one point to another in three-variable space in a simple manner as follows. We assume that the concentrations of drugs are constant and the decay rate of each cell population (L, Treg, Teff) is proportional only to the cell population ([L], [Treg], [Teff]) during induction chemotherapy. The rate constants of decay due to apoptosis and drugs are accordingly combined together as dL, dTreg, and dTeff during chemotherapy. Hematopoietic cell transplantation (HCT) or CTL infusion and Treg targeting as immunotherapy was modeled by instantaneous increases and decreases in [Teff] and [Treg], respectively.

The above model is translated into the following ordinary differential equations.

$$\frac{d[L]}{dt} = a_L\left(\frac{k_1^p}{k_1^p + [T_{eff}]^p}\right) - d_L[L] \qquad 1.1$$

$$\frac{d[T_{eff}]}{dt} = a_{T_eff}\left(\frac{k_2^p}{k_2^p + [T_{reg}]^p}\right) - d_{T_{eff}}[T_{eff}] \qquad 1.2$$

$$\frac{d[T_{reg}]}{dt} = a_{T_{reg}}\left(\frac{[L]^p}{k_3^p + [L]^p}\right) - d_{T_{reg}}[T_{reg}] \qquad 1.3$$

2.2 Parameter estimation and simulation

Some parameters in Eq. (1) were estimated using Bayesian inference via a Markov chain Monte Carlo (MCMC) technique with clinical data for lymphocyte recovery after induction chemotherapy, which is described in the Results section below. We implemented PROC MCMC in SAS v.9.4 (SAS Institute, Cary, NC). PROC MCMC solved the ordinary differential equation defined in PROC FCMP and we used the resulting solution in the construction of the likelihood function. In MCMC PROC, the unknown parameters were modeled using random effects to account for time-series variability as follows: exp(β+α) where β denotes the fixed-effects parameter and α denotes the random-effects parameter with an unknown covariance matrix. Normal priors were used for β with N(0,10). The MCMC simulations were run for 20000 iterations and the first 1000 were considered burnin and removed.

Steady states of the model were determined as the intersection of three nullclines (d[L]/dt = 0,

d[Teff]/dt = 0 and d[Treg]/dt = 0), which were numerically solved using the nleqslv R-package [36]. The ordinary differential equations in Eqs. 1.1, 1.2, and 1.3 were numerically solved using ODE solvers from MATLAB (Ver. 7.13; The Mathworks, Inc.).

3. Results

Using the MCMC technique, we parameterized the model using clinical data reported by Kanakry et al. [37]. They reported the kinetics of early lymphocyte recovery after intensive induction timed sequential therapy for AML and examined the immunophenotypic profile of the recovering lymphocytes. A median of 73% of the lymphocytes were CD3+ cells, which were composed of 16.7% CD3+CD4+ cells and 66.4% CD3+CD8+ cells. They reported that the median ratio of CD3+CD4+ cells to CD3+CD8+ cells was 2.7:1 and regulatory T cells characterized by CD3+CD4+ subpopulation expressing Foxp3 constituted 10.5% of CD3+CD4+ cells. We estimated cell numbers of regulatory T cells and CTLs characterized by CD3+CD8+ expression at each time point in the time course of lymphocyte recovery presented by Kanakry et al., with the assumption that the above immunophenotypic profile is not changed during early lymphocyte recovery after intensive chemotherapy.

Assuming that [L] is approximately to be a constant [L]ss during complete remission (CR) after intensive induction chemotherapy, the model to be calibrated is Equations 1.2 and 1.3 with [L]ss. While < 5% leukemic blast cells among the total population of nucleated cells in bone marrow is included in the criteria for CR in AML, there is no definitive criterion for the peripheral blast count at CR. According to the clinical observation that 0% to 5% peripheral blast cells at CR had no effect on relapse free survival (RFS) time [38], we selected 100/μL for [L]ss during CR with 1% peripheral blast cells and 10000/μL as normal counts of peripheral nucleated cells.

Estimated means and standard deviations of β for aTeff, aTreg, dTeff and dTreg by the MCMC method are 4.03±0.47, 5.29±1.08, -1.60±0.78 and -3.23±2.74, respectively. The time courses of [Teff] and [Treg] obtained by numerical integration of Equations 1.2 and 1.3 with aTeff=56.53, aTreg=198.2, dTeff=0.2 and dTreg=0.04 as exp(means) are shown in Fig. 2, together with counts of CD3+CD8+ cells (CTLs) and CD3+CD4+Foxp3+ cells (regulatory T cells) estimated from lymphocyte recovery after induction chemotherapy reported by Kanakry et al. [37].

Dependencies of the steady-state concentrations of L, Teff, and Treg on the parameter k2, k3 and p reveal two stable steady states corresponding to high and low concentrations accompanied by one unstable steady state with intermediate concentrations, as shown in Fig. 3. While keeping the parameters aTreg, aTeff, dTreg, and dTeff to estimated values by the MCMC method, we searched a wide range of the parameter space of aL, dL, k1 and found parameter ranges characterized by the existence of one or two stable steady states separated by an unstable fixed point. The values of k2, k3 and p were set within the parameter ranges of bistability. However, we cannot exclude the

existence of different dynamics, such as a limit cycle. The values of model parameters in the present study are listed in Table 1.

We assume that the two stable steady states correspond to the state (SShi) of high leukemic cell load at diagnosis or relapse and the state (SSlo) of low leukemic cell load at long-term complete remission. In our simulations, the transitions from SShi to SSlo or the return to original SShi, which are induced by hypothetical chemotherapy and immunotherapy, were visualized as dynamical trajectories in three-dimensional space defined by the concentrations of L, Teff, and Treg.

Fig. 4a shows the trajectories from SShi ([L], [Teff], [Treg] = 100000/μL, 0.00031/μL, 4955/μL, out of figure) for chemotherapy with different values of dL. The locations of the state produced by chemotherapy shift toward SSlo ([L], [Teff], [Treg] = 40/μL, 283/μL, 8/μL) with increasing dL and determine whether the system reaches SSlo or returns to the original SShi. It is found that there are two basins of attraction in which the trajectories converge to SSlo and back to the original SShi. It is noted that the returning trajectories close to the boundary are attractive towards SSlo, compared with repulsive trajectories far from the boundary. Fig. 4b shows time courses corresponding to the returning trajectories. This indicates that the system spends considerable time in the vicinity of the boundary before returning to SShi. In Fig. 5, the state points leading to SShi are denoted by dots and those leading to SSlo are not marked, suggesting two basins of attraction. The latter can be seen as a blank region. It is noted that larger dots from which the system spends longer before returning to SShi are distributed along the boundary. We propose that transient CR with longer duration could be interpreted as having such transient dynamics [39] before returning to SShi, which could be considered in the framework of the resilience of dynamical systems [25].

There has been considerable interest in targeting Treg-mediated suppression of anti-AML reactive T cells. Bachanova et al. focused on the impact of prior Treg depletion followed by anti-leukemic cell infusion [40]. Patients with refractory AML received Treg depletion with IL-2 diphtheria toxin (IL2DT), which can selectively deplete IL-2 receptor-expressing cells, including Tregs. We simulated the impact of prior Treg depletion followed by Teff infusion. Teff infusion and Treg targeting were modeled by instantaneous modulations of [Teff] and [Treg] after hypothetical chemotherapy. An example is shown in Fig. 6. The returning trajectory to SShi after chemotherapy split into two trajectories. One is due to decreases in [Treg] followed by increases in [Teff] leading to SSlo. Another is due to only increases in [Teff], leading to the original SShi. The difference is due to whether or not the system crosses the basin boundary.

4. Discussion

The present model comprising L, Teff, and Treg, including promotion of Treg production by

L, exhibits two coexisting, stable steady states (SShi and SSlo) with a given parameter set. Assuming that SShi and SSlo correspond to the state at diagnosis or relapse and the state of long-term complete remission, the effects of hypothetical chemotherapy and immunotherapy inducing the transition from SShi to SSlo and returning to SShi are visualized as trajectories in three-dimensional space defined by L, Teff, and Treg concentrations.

Our results demonstrate that there is, in three-dimensional space, a boundary between two basins of attraction of SShi and SSlo, and that effective treatments move the trajectory to the basin of attraction of SSlo. That is, given the existence of the boundary, the strategy of treatment design leads to how the trajectory from SShi is forced to exceed the boundary and reach the region in which all states begin their trajectories converging to SSlo. This viewpoint is in line with an ecological resilience perspective on cancer [41]. Some mathematical models of cancer and immune cells interplay exhibit multistable steady states and were used to investigate the effectiveness of state transitions between the basins of attraction by the combination of hypothetical immunotherapy with chemotherapy [42,43] or radiation therapy [44]. Our model, which incorporates positive feedback between regulatory T cells and leukemic cells, also shows bistability with two basins of attraction, which serve as a framework for assessing extensive studies of immunotherapy targeting regulatory T cells of immunosuppressive activity and design of combined immunotherapy with chemotherapy. The predictions that flow from the putative existence of the basin boundary are the effectiveness of Teff infusion/Treg depletion and the effect of the number of infused cells exceeding the boundary in three-dimensional space. These predictions remain to be evaluated by clinical studies of immunotherapy.

The existence of the boundary suggested by this work may be supported by the findings of clinical studies of minimal residual disease (MRD) monitoring in leukemia. During CR attained with induction chemotherapy and maintenance treatment, submicroscopic amounts of residual leukemic cells in peripheral blood and bone marrow could not be identified cytomorphologically but could be sensitively detected by multiparameter flow cytometry (MFC) and quantitative real-time polymerase chain reaction (RT-qCR) in MRD monitoring [45,46]. Liu Yin et al. reported that RUNX1-RUNX1T1 and CBFB-MYH11 fusion transcripts during CR in patients with core binding factor (CBF) positive AML were quantified by qPCR for bone marrow (BM) and peripheral blood (PB) samples [28]. They identified MRD thresholds predicting whether cytomorphologically-detectable hematologic relapse occurs: hematologic relapse was 100% in patients with more than 500 RUNX1-RUNX1T1 copies in BM and more than 100 copies in PB, compared with 7% in patients with fewer than 500 copies and 7% in patients with fewer than 100 copies respectively, and 100% in patients with more than 50 CBFB-MYH11 copies in BM and 97% in patients with more than 10 copies in PB, compared with 10% in patients with fewer than 50 copies in BM and 7% in patients with fewer than 10 copies in PB respectively [28]. Several studies also reported MRD thresholds as independent

prognostic factors for predicting relapse occurrence in AML [47-49]. The MRD threshold can therefore be explained from the existence of the boundary found in our model.

We propose that transient CR before relapse with longer duration corresponds to the case in which the system spends longer near the boundary before returning to SShi. This leads to the prediction that longer duration of CR achieved by induction and consolidation chemotherapy is a favorable factor for outcomes of the subsequent chemotherapy and HCT or infusion of purified effector cells at relapse, as lower-dose chemotherapy or lower load of effector cells is needed for the system located near the boundary to exceed it and converge to SSlo. Our prediction is in line with better outcomes achieved by chemotherapy [50,51] and HCT [52] for relapsing patients with longer duration of first CR. The distribution of CR duration could be simulated with a threshold defining CR and be translated to a relapse free survival (RFS) curve. The simulated RFS curves could be directly compared with clinical outcomes in treatments of AML, resulting in the validation of our model to predict the impact of chemotherapy and immunotherapy for AML.

Another aspect of the trajectory crossing near the boundary is the accompanying transient increase in Teff concentration as shown in Fig. 4a. This leads to the prediction that higher absolute lymphocyte count (ALC) recovery is observed during CR with longer duration and is associated with a survival advantage for patients, which may be supported by ALC being identified as an independent prognostic factor for survival [53].

With our viewpoint of transient CR corresponding to the trajectory returning to SShi in three-dimensional space, relapse occurs without a change of parameter sets, in which coexisting stable steady states (SShi and SSlo) appear as shown in Fig. 3. On the other hand, assuming that the change of parameter values in our model is due to gene mutations during disease progression, the alternative explanation for relapse is possible. If the value of k2 decreases beyond the point of the bifurcation in Fig. 3a, the system remaining at SSlo is forced to go to SShi.

In summary, the dynamics of this model qualitatively explain some clinical findings of AML. Our model, which is yet to be further assessed against clinical data, may provide valuable information for the future design of combined immunotherapy with chemotherapy in AML.

Acknowledgements

We thank Mr. Tony Atkinson for his critical reading and advice on the manuscript. We also thank the referees for their valuable suggestions.

References

[1] U.Y. Malkan, G.G. Ayse, I.E. Eliacik, S. Etgul, T. Aslan, et al., Rebound thrombocytosis following induction chemotherapy is an independent predictor of a good prognosis in acute myeloid leukemia patients attaining first complete remission, Acta Haematol. 134(2015)32-37.

[2] M. Yanada, G. Borthakur, G. Garcia-Manero, F. Ravandi, S. Faderl, S. Pierce, et al., Blood counts at time of complete remission provide additional independent prognostic information in acute myeloid leukemia, Leuk Res. 32(10)(2008)1505-1509.

[3] C. Ustun, J.S. Miller, D.H. Munn, D.J. Weisdorf, B.R. Blazar, Regulatory T cells in acute myelogenous leukemia: is it time for immunomodulation? Blood 118(19)(2011)5084-5095.

[4] S. Lindley, C.M. Dayan, A. Bishop, B.O. Roep, M. Peakman, T.I.M. Tree, Defective suppressor function in CD4(+)CD25(+) T-cells from patients with type 1 diabetes, Diabetes. 54(1)(2005)92–99.

[5] R.J. DiPaolo, C. Brinster, T.S. Davidson, J. Andersson, D. Glass, E.M. Shevach, Autoantigen-specific TGFβ-induced Foxp3+ regulatory T cells prevent autoimmunity by inhibiting dendritic cells from activating autoreactive T cells, J Immunol. 179(7)(2007)4685–4693.

[6] C. Riether, C.M. Schurch, A.F. Ochsenbein, Regulation of hematopoietic and leukemic stem cells by the immune system, Cell Death and Differ. 22(2015)187-198.

[7] Z. Shenghui, H. Yixiang, W.Jianbo, Y. Kang, B. Laixi, Z. Yan, X. Xi, Elevated frequencies of CD4+CD25+CD127lo regulatory T cells is associated to poor prognosis in patients with acute myeloid leukemia, Int. J. Cancer 129(6)(2011)1373-1381.

[8] M.J. Szczepanski, M. Szajnik, M. Czystowska, M. Mandapathil, L. Strauss, A. Welsh, et al., Increased frequency and suppression by regulatory T cells in patients with acute myelogenous leukemia, Clin. Cancer Res. 15(10)(2009)3325-3332.

[9] E. Ersvaer, K. Liseth, J. Skavland, B.T. Gjertsen, Ø. Bruserud, Intensive chemotherapy for acute myeloid leukemia differentially affects circulating TC1, TH1, TH17 and TREG cells, BMC Immunol. 11(38)(2010).

[10] W. Yang, Y. Xu Clinical significance of Treg cell frequency in acute myeloid leukemia, Int. J. Hematol. 98(5)(2013)558-562.

[11] M.C. Mackey, C. Ou, L. Pujo-Menjouet, J. Wu, Periodic oscillations of blood cell populations in chronic myelogenous leukemia, SIAM J. Math. Anal. 38(1)(2006)166-187.

[12] D. Wodarz, N. Garg, N.L. Komarova, O. Benjamini, M.J. Keating, W.G. Wierda, et al., Kinetics of CLL cells in tissues and blood during therapy with the BTK inhibitor ibrutinib, Blood 123(26)(2014)4132-4135.

[13] F. Michor, T.P. Hughes, Y. Iwasa, S. Branford, N.P. Shah, C.L. Sawyers, M.A. Nowak,

Dynamics of chronic myeloid leukemia, Nature 435(7046)(2005)1267-1270.
[14] I. Roeder, M. Horn, I. Glauche, A. Hochhaus, M.C. Mueller, M. Loeffler, Dynamic modeling of imatinib-treated chronic myeloid leukemia: functional insights and clinical implications, Nature Med. 12(10)(2006)1181-1184.
[15] A.L. MacLean, S. Filippi, M.P. Stumpf, The ecology in the hematopoietic stem cell niche determines the clinical outcome in chronic myeloid leukemia, Proc. Natl. Acad. Sci. USA 111(10)(2014)3883-3888.
[16] T. Stiehl, N. Baran, A.D. Ho, A. Marciniak-Czochra, Cell division patterns in acute myeloid leukemia stem-like cells determine clinical course: a model to predict patient survival, Cancer Res. 75(6)(2015)940-949.
[17] V.A. Kuznetsov, I.A. Makalkin, M.A. Taylor, A.S. Perelson, Nonlinear dynamics of immunogenic tumors: parameter estimation and global bifurcation analysis, Bull. Math. Biol. 56(2)(1994)295–321.
[18] P.S. Kim, P.P. Lee, D. Levy, Dynamics and potential impact of the immune response to chronic myelogenous leukemia, PLoS Computational Biol. 4(6)(2008)e1000095.
[19] K. Roesch, D. Hasenclever, M. Scholz, Modelling lymphoma therapy and outcome, Bull. Math. Biol. 76(2)(2014)401-430.
[20] T.S. Gardner, C.R. Cantor, J.J. Collins, Construction of a genetic toggle switch in Escherichia coli, Nature 403(6767)(2000)339-342.
[21] D. Angeli, J.E. Ferrell, E.D. Sontag, Detection of multistability, bifurcations, and hysteresis in a large class of biological positive-feedback systems, Proc. Natl. Acad. Sci. USA 101(7)(2004)1822-1827.
[22] J.J. Tyson, R. Albert, A. Goldbeter, P. Ruoff, J. Sible, Biological switches and clocks, J. R. Soc. Interface 5(Suppl 1)(2008)S1–S8.
[23] J.E. Ferrell Jr., Bistability, bifurcation, and Waddington's epigenetic landscape, Curr. Biol. 22(11)(2012)R458-R466.
[24] L. Wanga, B.L. Walkera, S. Iannacconeb, D. Bhatta, P.J. Kennedya, W.T. Tse, Bistable switches control memory and plasticity in cellular differentiation, Proc. Natl. Sci. USA 106(16)(2009)6638-6643.
[25] K.Meyer, A mathematical review of resilience in ecology, Natural Resource Modeling, 29(3)(2016)339-352.
[26] E. Estey, Treatment of refractory AML, Leukemia 10(6)(1996)932-936.
[27] F.V. Michelis, E.G. Atenafu, V. Gupta, D.D. Kim, J. Kuruvilla, A. Lambie, et al., Duration of first remission, hematopoietic cell transplantation-specific comorbidity index and patient age predict survival of patients with AML transplanted in second CR, Bone Marrow Transplant. 48(11)(2013)1450-1455.

[28] J.A. Liu Yin, M.A. O'Brien, R.K. Hills, S.B. Daly, K. Wheatley, A.K. Burnett, Minimal residual disease monitoring by quantitative RT-PCR in core binding factor AML allows risk stratification and predicts relapse: results of the United Kingdom MRC AML-15 trial, Blood 120(2012)2826-2835.
[29] C. Schürch, C. Riether, M.A. Amrein, A.F. Ochsenbein, Cytotoxic T cells induce proliferation of chronic myeloid leukemia stem cells by secreting interferon-γ, J. Exp. Med. 210(2013)605-621.
[30] W.J. Norde, I.M. Overes, F. Maas, H. Fredrix, J.C. Vos, M.G. Kester, R. van der Voort, I. Jedema, J.H. Falkenburg, A.V. Schattenberg, T.M. de Witte, H. Dolstra, Myeloid leukemic progenitor cells can be specifically targeted by minor histocompatibility antigen LRH-1-reactive cytotoxic T cells, Blood 113(2009)2312-2323.
[31] S. Shen, Yi Ding, C.E. Tadokoro, D. Olivares-Villagómez, M. Camps-Ramírez, M.A.C. de Lafaille, J.J. Lafaille, Control of homeostatic proliferation by regulatory T cells, J. Clin. Invest. 115(2005)3517-3526.
[32] A. McNally, G.R. Hill, T. Sparwasser, R. Thomas, R.J. Steptoe, CD4+CD25+ regulatory T cells control CD8+ T-cell effector differentiation by modulating IL-2 homeostasis, Proc. Natl. Acad. Sci. USA 108(2011)7529-7534.
[33] A. Curti, S. Pandolfi, B. Valzasina, M. Aluigi, A. Isidori, E. Ferri, et al., Modulation of tryptophan catabolism by human leukemic cells results in the conversion of CD25- into CD25+ T regulatory cells, Blood 109(7)(2007)2871-2877.
[34] L.M. Francisco, V.H. Salinas, K.E. Brown, V.K. Vanguri, G.J. Freeman, V.K. Kuchroo, A.H. Sharpe, PD-L1 regulates the development, maintenance, and function of induced regulatory T cells, J. Exp. Med. 206(13)(2009)3015-3029.
[35] S.J. Coles, R.K. Hills, E.C. Wang, A.K. Burnett, S. Man, R.L. Darley, A.Tonks, Increased CD200 expression in acute myeloid leukemia is linked with an increased frequency of FoxP3+ regulatory T cells, Leukemia 26(9)(2012)2146-2148.
[36] B. Hasselman, nleqslv: Solving systems of non linear equations, R package version 2.1.1(2014).
[37] C.G. Kanakry, A.D. Hess, C.D.Gocke, C. Thoburn, F. Kos, C. Meyer, et al., Early lymphocyte recovery after intensive timed sequential chemotherapy for acute myelogenous leukemia: peripheral oligoclonal expansion of regulatory T cells, Blood 117(2)(2011)608-617.
[38] E.H.Estey, P.F.Thall, X.Wang, S.Verstovsek, J.Cortes, H.M.Kantarjian, Effect of circulating blasts at time of complete remission on subsequent relapse-free survival time in newly diagnosed AML, Blood 102(2003)3097-3099.
[39] J. Jaeger, D. Irons, N. Monk, The inheritance of process: a dynamical systems approach, J. Exp. Zool. B Mol. Dev. Evol. 318(8)(2012)591-612.
[40] V.Bachanova, S.Cooley, T.E.Defor, M.R.Verneris, B.Zhang, D.H.McKenna, J.Curtsinger, A.Panoskaltsis-Mortari, D.Lewis, K.Hippen, P.McGlave, D.J.Weisdorf, B.R.Blazar, J.S.Miller, Clearance of acute myeloid leukemia by haploidentical natural killer cells is improved using IL-2

diphtheria toxin fusion protein, Blood 123(25)(2014)3855-3863.
[41]A.C.Fassoni and H.M.Yang, An ecological resilience perspective on cancer: insights from a toy model, Ecological Complexity 30(2017)34-46.
[42] L.G. de Pillis, W. Gu, A.E. Radunskaya, Mixed immunotherapy and chemotherapy of tumors: modeling, applications and biological interpretations, Journal of theoretical Biology 238 (2006) 841-862.
[43] L.G. De Pillis, A. Radunskaya, A mathematical tumor model with immune resistance and drug therapy: an optimal control approach, Journal of Theoretical Medicine, 3(2001)841-862.
[44] M. Lu, B. Huanga, S.M. Hanash, J.N. Onuchica, E. Ben-Jacob, Modeling putative therapeutic implications of exosome exchange between tumor and immune cells, Proc. Natl. Acad. Sci. USA, 22(2014)E4165-E4174.
[45] W. Kern, C. Schoch, T. Haferlach, S. Schnittger, Monitoring of minimal residual disease in acute myeloid leukemia, Critical Reviews in Oncology/Hematology, 56 (2005) 283-309.
[46] S. Kayser, A. Benner, C. Thiede, U. Martens, J. Huber, P. Stadtherr, J.W.G. Janssen, C. Röllig, M.J. Uppenkamp, T. Bochtler, U. Hegenbart, G. Ehninger, A.D. Ho, P. Dreger, A. Krämer, Pretransplant NPM1 MRD levels predict outcome after allogeneic hematopoietic stem cell transplantation in patients with acute myeloid leukemia, Blood Cancer Journal 6(2016)e449.
[47] W. Zeijlemaker, A. Kelder, Y.J.M. Oussoren-Brockhoff, W.J. Scholten, A.N. Snel, D. Veldhuizen, J. Cloos, G.J. Ossenkoppele, G.J. Schuurhuis, Peripheral blood minimal residual disease may replace bone marrow minimal residual disease as an immunophenotypic biomarker for impending relapse in acute myeloid leukemia, Leukemia 30(2016)708-715.
[48] T. Kohnke, D. Sauter, K. Ringel, E. Hoster, R.P. Laubender, M. Hubmann, S.K. Bohlander, P.M. Kakadia, S. Schneider, A. Dufour, M.C. Sauerland, W.E. Berdel, T. Buchner, B. Wormann, J. Braess, W. Hiddemann, K. Spiekermann, M. Subklewe, Early assessment of minimal residual disease in AML by flow cytometry during aplasia identifies patients at increased risk of relapse, Leukemia 29(2015)377-386.
[49] V.H.J. van der Velden, A. van der Sluijs-Geling, B.E.S. Gibson, J.G. te Marvelde, P.G. Hoogeveen, W.C.J. Hop, K. Wheatley, M.B. Bierings, G.J. Schuurhuis, S.S.N. de Graaf, E.R. van Wering, J.J.M. van Dongen, Clinical significance of flowcytometric minimal residual disease detection in pediatric acute myeloid leukemia patients treated according to the DCOG ANLL97/MRC AML12 protocol, Leukemia 24(2010)1599-1606.
[50] W. Hiddemann, W.R. Martin, C.M. Sauerland, A. Heinecke, T.Büchner, Definition of refractoriness against conventional chemotherapy in acute myeloid leukemia: a proposal based on the results of retreatment by thioguanine, cytosine arabinoside, and daunorubicin (TAD 9) in 150 patients with relapse after standardized first line therapy, Leukemia 4(3)(1990)184-188.
[51] E.H. Estey, Treatment of relapsed and refractory acute myelogenous leukemia, Leukemia

14(3)(2000)476-479.
[52] F.V. Michelis, E.G. Atenafu, V. Gupta, D.D. Kim, J. Kuruvilla, A. Lambie, et al., Duration of first remission, hematopoietic cell transplantation-specific comorbidity index and patient age predict survival of patients with AML transplanted in second CR, Bone Marrow Transplant. 48(11)(2013)1450-1455.
[53] D. Behl, L.F. Porrata, S.N. Markovic, L. Letendre, R.K. Pruthi, C.C. Hook, et al., Absolute lymphocyte count recovery after induction chemotherapy predicts superior survival in acute myelogenous leukemia, Leukemia 20(1)(2006)29-34.

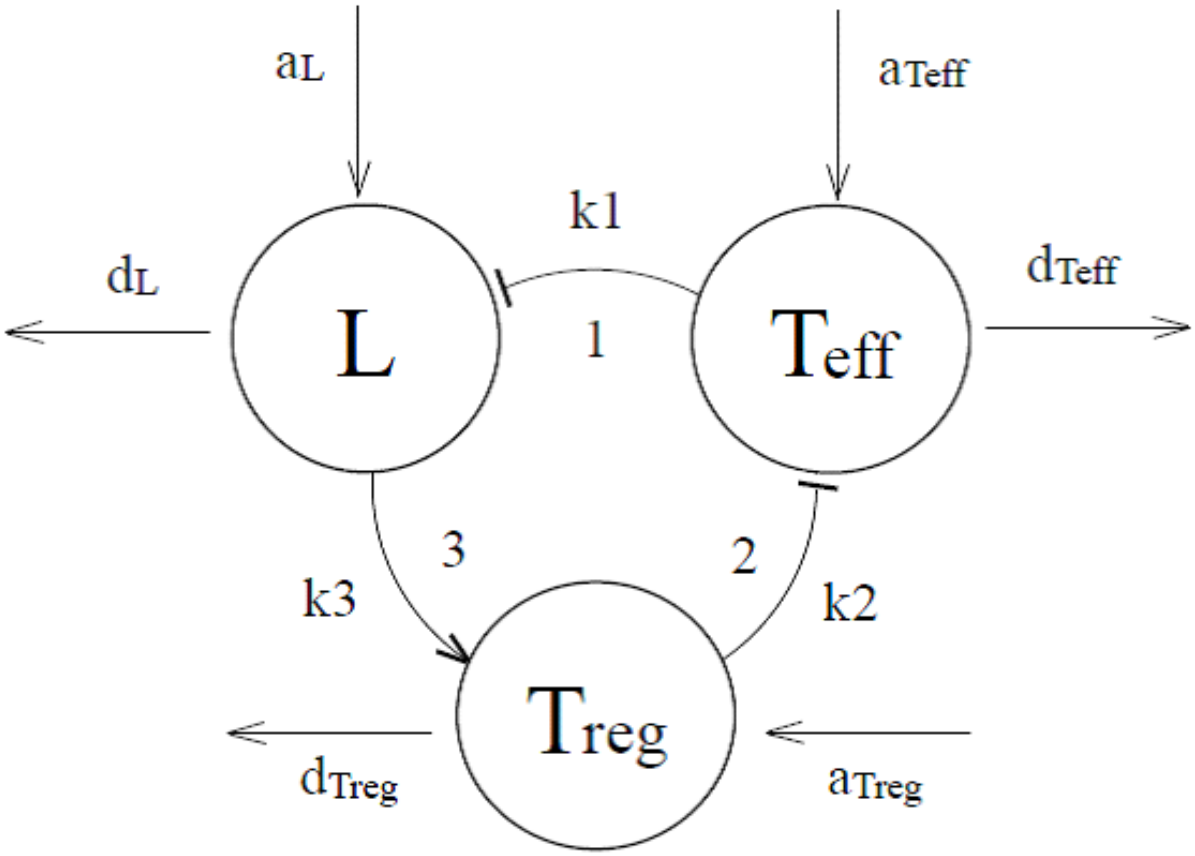

Fig. 1: Mechanistic model for crosstalk among leukemic cells and immune cells in AML. The processes of cell-cell interaction are numbered as follows: 1. Leukemic stem cells and progenitor cells targeted by effector T cells, 2. Effector T cell suppression mediated by Treg, and 3. Treg formation promoted by leukemic blast cells (L).

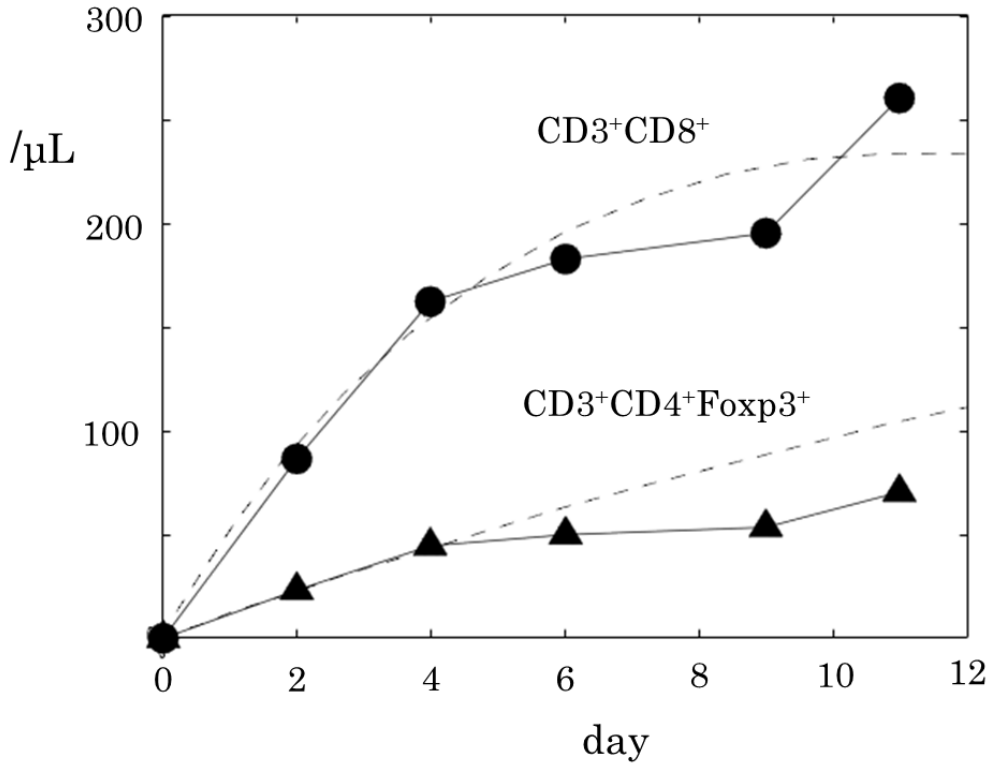

Fig. 2: Time courses of counts of CD3+CD8+ cells (CTLs, closed circles) and CD3+CD4+Foxp3+ cells (regulatory T cells, closed triangles) estimated from lymphocyte recovery after induction chemotherapy reported by Kanakry et al. [37]. Dashed lines show time courses of [Teff] and [Treg] obtained by numerical integration of Eqs 1.2 and 1.3 with aTeff=56.53, aTreg=198.2, dTeff=0.2 and dTreg=0.04 estimated by an MCMC technique.

Symbol	Value
cell influx	
a_L	0.1 - 1000 $\mu L^{-1} day^{-1}$
a_{Teff}	56.53 $\mu L^{-1} day^{-1}$
a_{Treg}	198.2 $\mu L^{-1} day^{-1}$
cell decay	
d_L	0.0001 - 1.0 day^{-1}
d_{Teff}	0.2 day^{-1}
d_{Treg}	0.04 day^{-1}
cell interaction	
k_1	1 - 1000 μL^{-1}
k_2	160 μL^{-1}
k_3	200 μL^{-1}
hill coefficient	
p	1-10

Table 1: Parameter Values Used in the Simulation

Fig. 3: Steady states as a function of the threshold constant k2 of a) leukemic blast cells (L), b) mature effective T cells (Teff), and c) mature regulatory T cells (Treg), and of the threshold constant k3 of d) leukemic blast cells (L), and of the Hill coefficient p of e) leukemic blast cells (L). Steady states along the solid lines are stable and steady states along dashed lines are unstable. Parameter ranges characterized by the existence of two stable steady states separated by an unstable fixed point are marked by gray backgrounds. Parameter values are aL=1000, aTeff=56.53, aTreg=198.2, dL=0.01, dTeff=0.2, dTreg=0.04, k1=40, k3=200, and p=4 for a), b), c) ,and aL=1000, aTeff=56.53, aTreg=198.2, dL=0.01, dTeff=0.2, dTreg=0.04, k1=40, k2=160, and p=4 for d), and aL=1000, aTeff=56.53, aTreg=198.2, dL=0.01, dTeff=0.2, dTreg=0.04, k1=40, k2=160, and k3=200 for e).

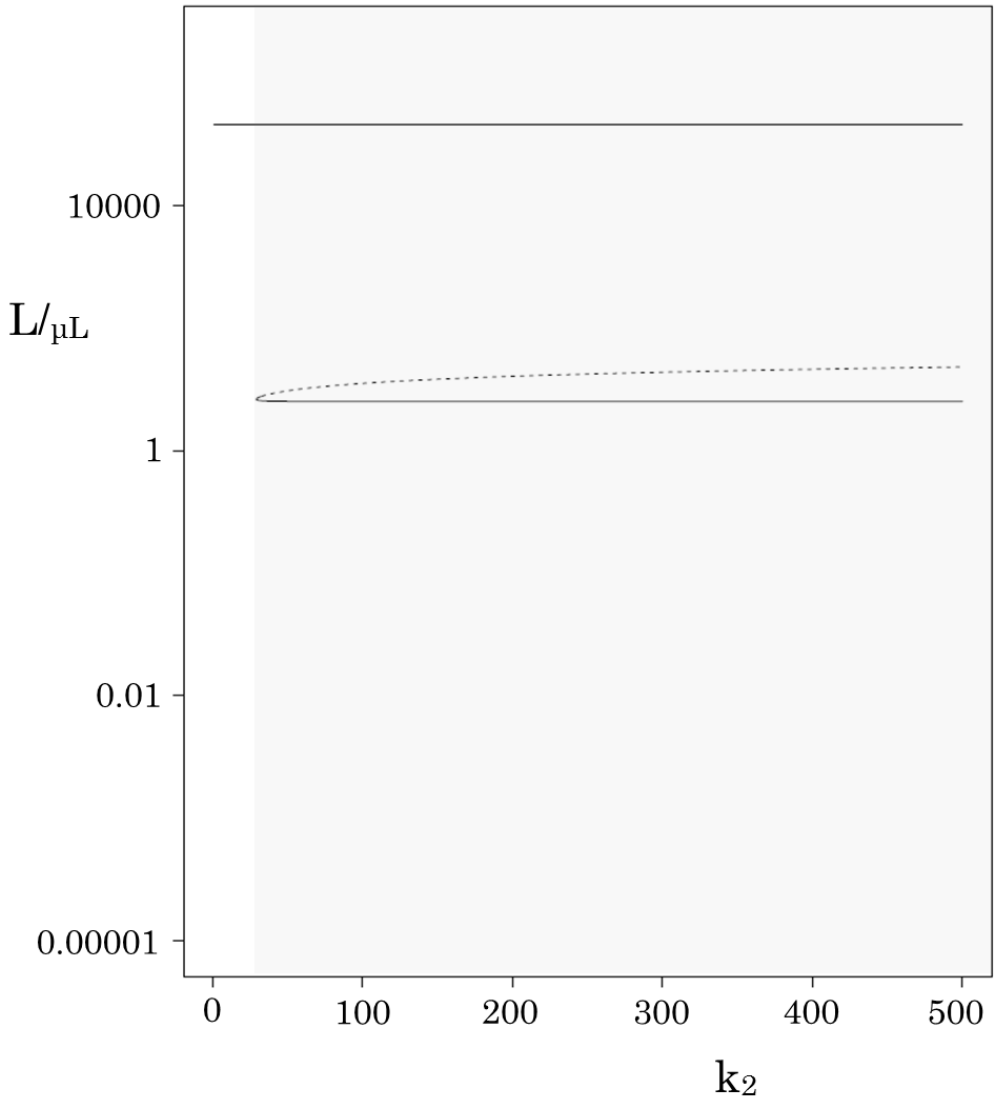

Fig. 3a

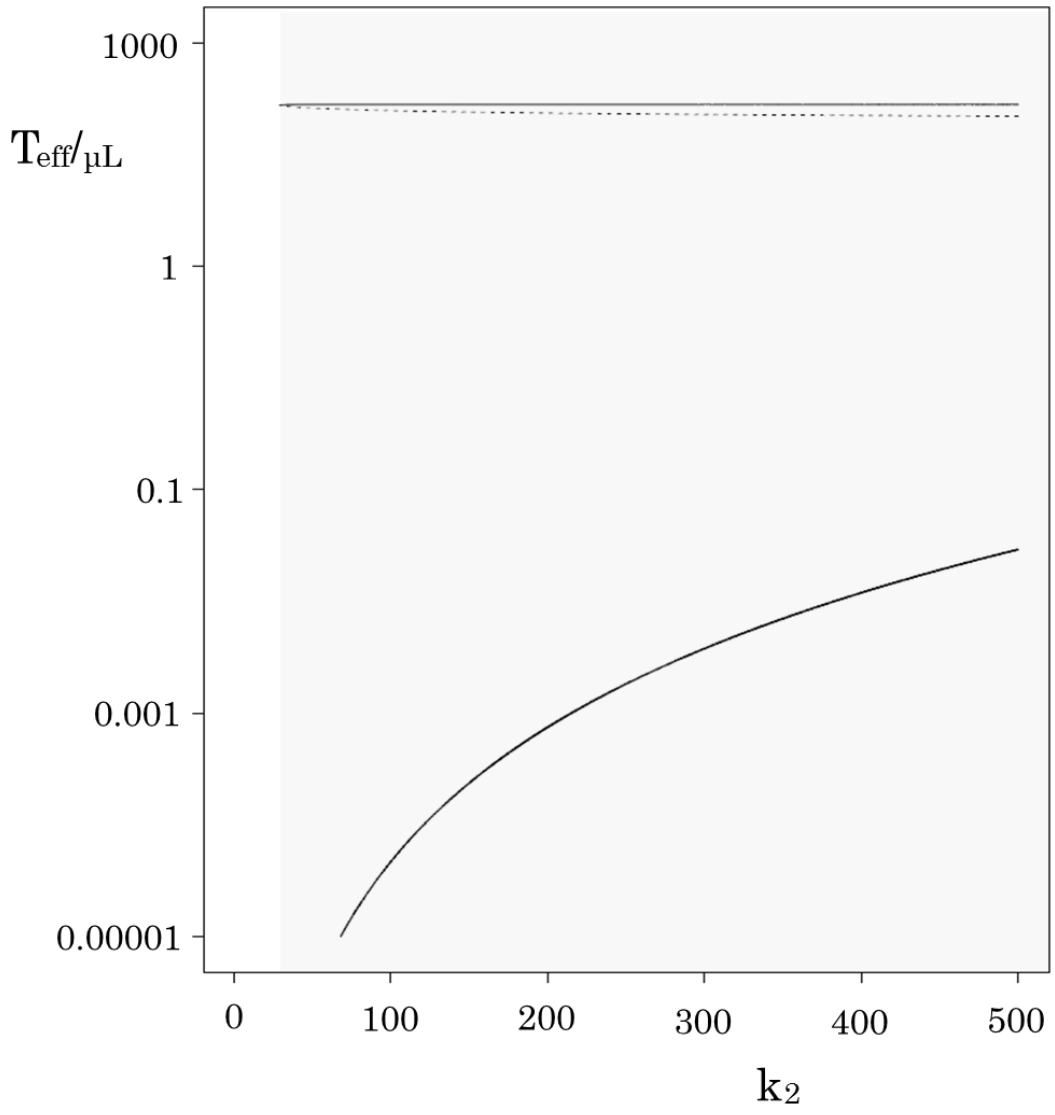

Fig. 3b

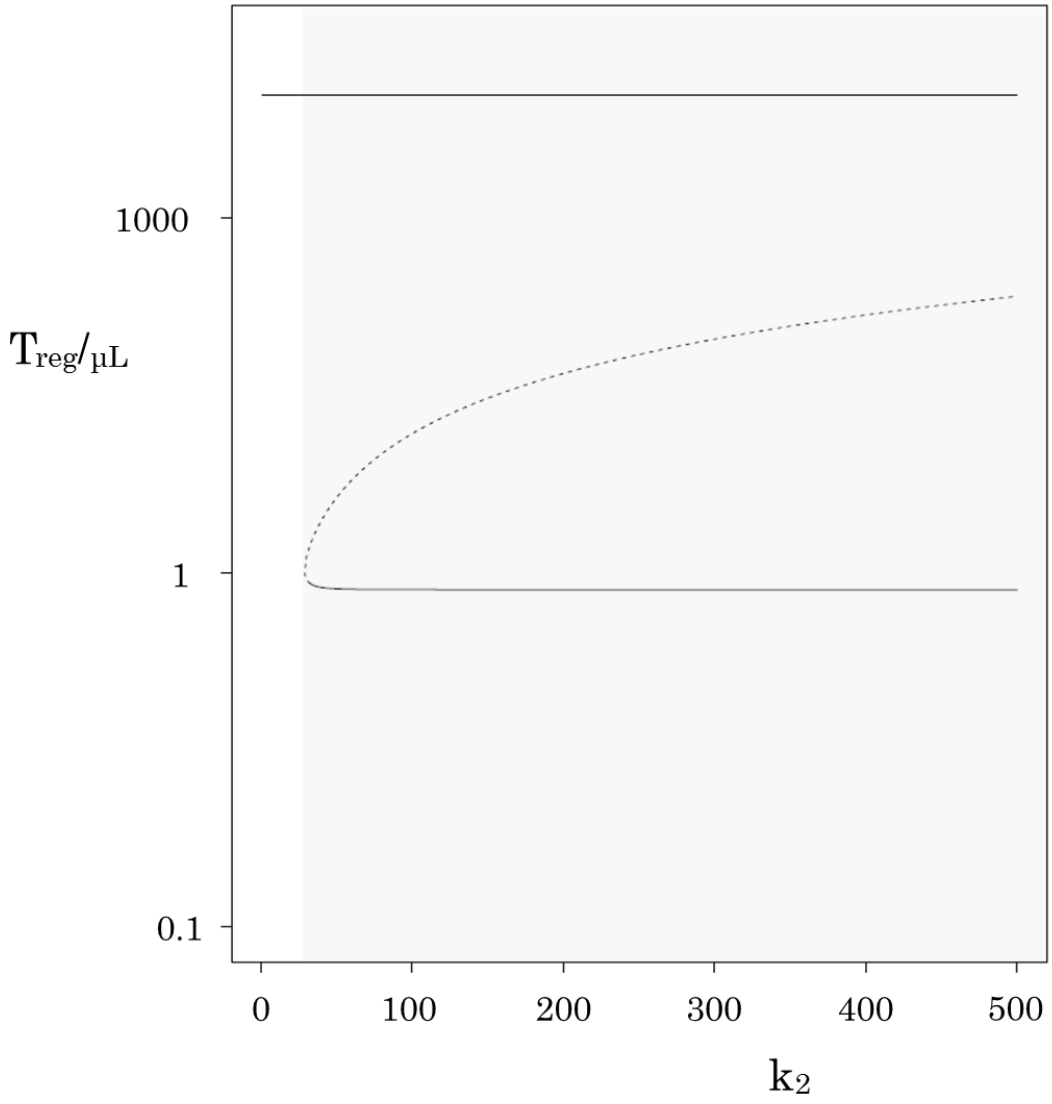

Fig. 3c

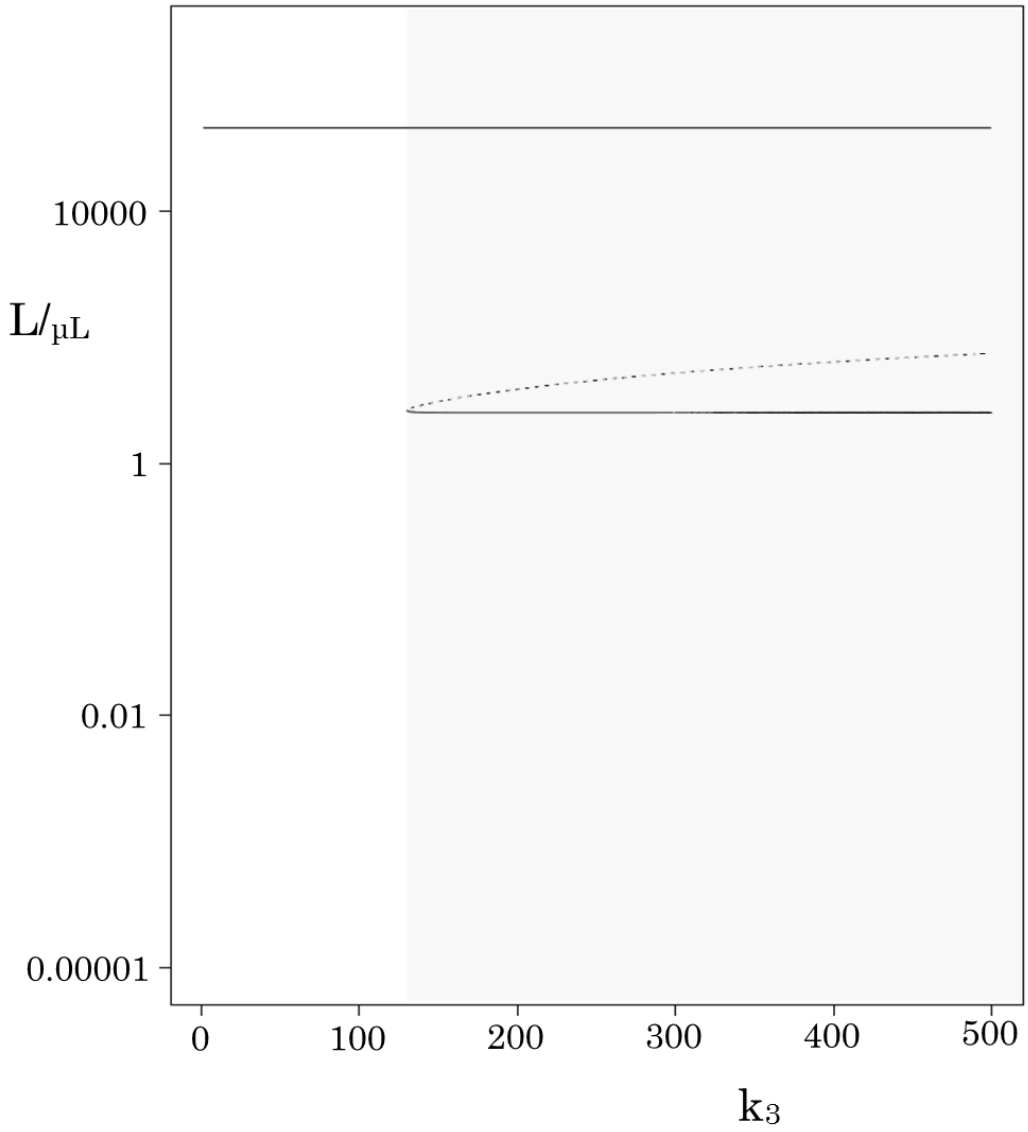

Fig.3d

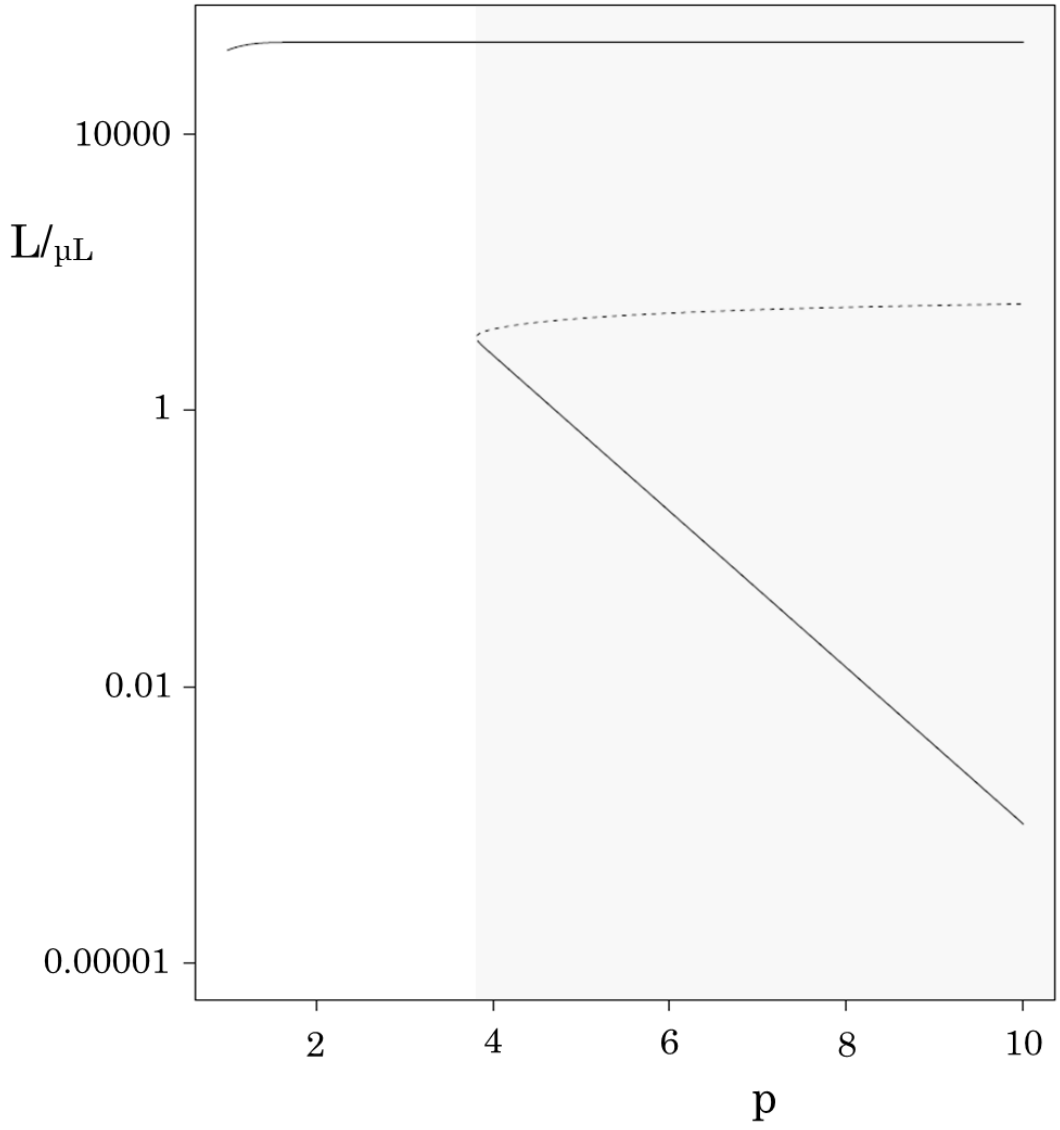

Fig. 3e

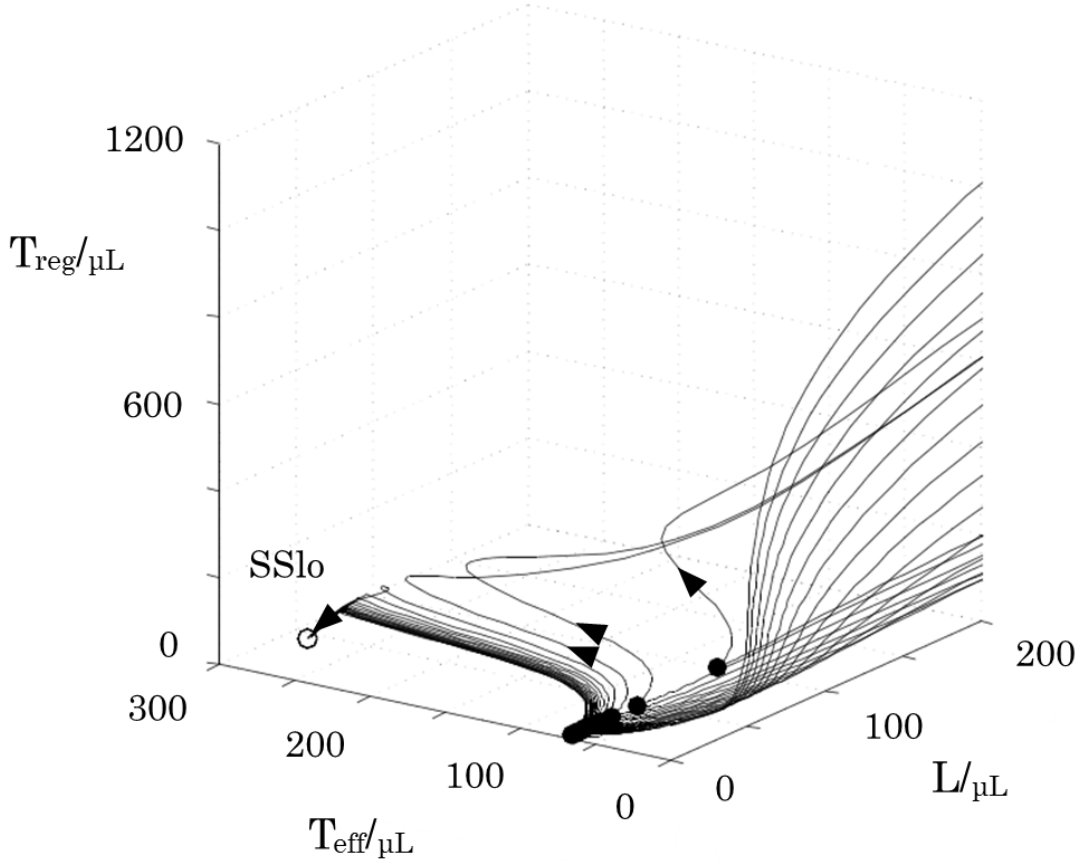

Fig. 4a: The trajectories from SShi (not shown in figure) after chemotherapy with different values of dL. The locations of the state produced by chemotherapy are denoted by closed circles. For higher dL, the trajectories with dL beyond a critical value change direction from returning to SShi to converging to SSlo, suggesting two basins of attraction. SShi ([L], [Teff], [Treg] = 100000/μL, 0.00031/μL, 4955/μL, out of figure) and SSlo ([L], [Teff], [Treg] = 40/μL, 283/μL, 8/μL, open circle in figure) were calculated with dL=0.01. Other parameter values are aL=1000, aTeff=56.53, aTreg=198.2, dTeff=0.2, dTreg=0.04, k1=40, k2=160, k3=200, and p=4. For a chemotherapy duration of 10 days, the decay rate constants were dTeff=0.8, dTreg=5.0, and dL was changed from 1.0 to 20.0.

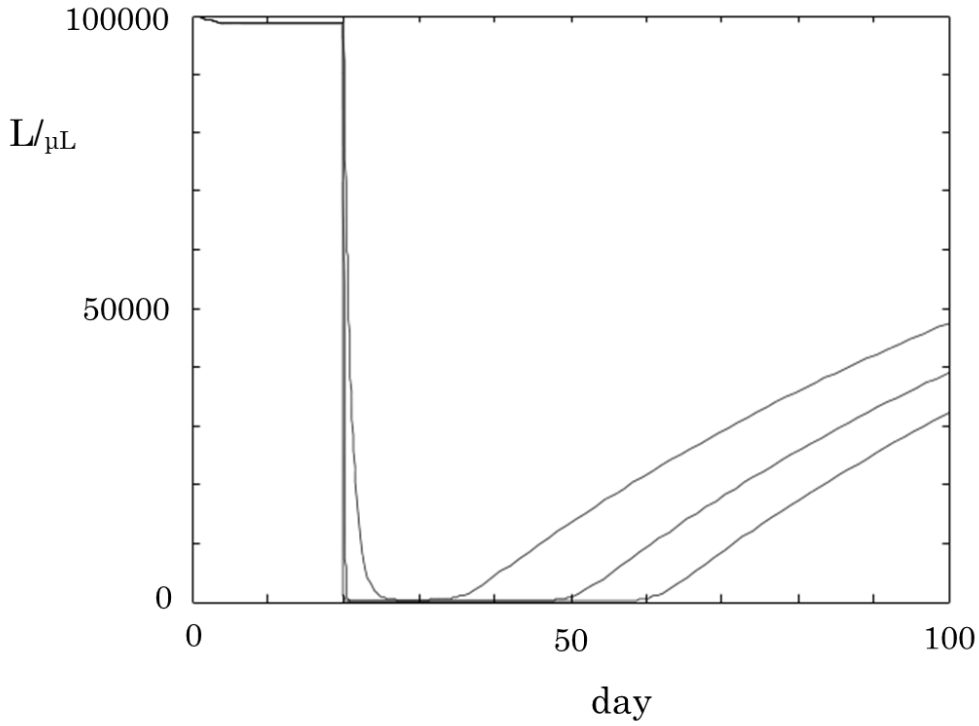

Fig. 4b: Time courses corresponding to the trajectories returning to SShi. The start of relapse is delayed with increasing dL. Parameter values are aL=1000, aTeff=56.53, aTreg=198.2, dL=0.01, dTeff=0.2, dTreg=0.04, k1=40, k2=160, k3=200, and p=4. For a chemotherapy duration of 10 days, the decay rate constants were dTeff=1.0, dTreg=5.0 and dL were 1.0, 10.0 and 100.0.

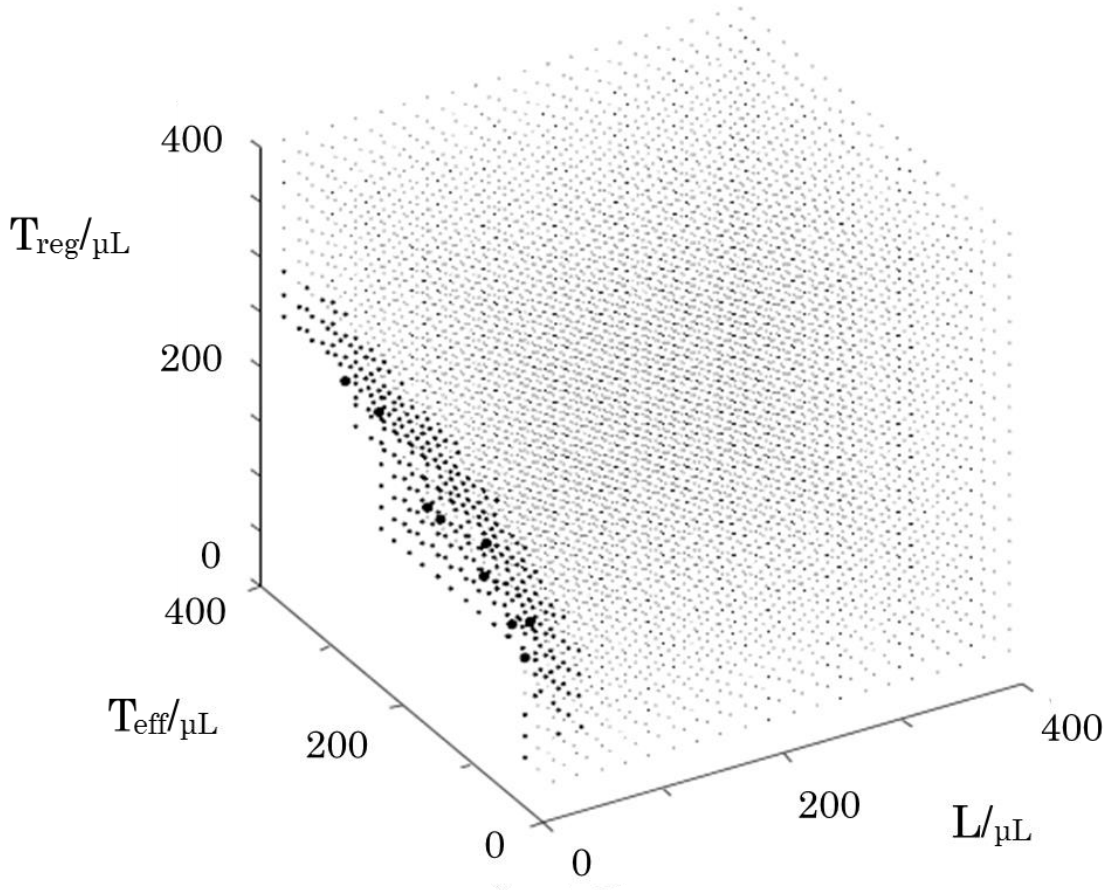

Fig. 5: The basin of attraction of SShi. The size of each dot in the basin indicates the time required for the system to arrive at SShi from the state denoted by a dot. It takes longer for the system to arrive at SShi from states distributed along the basin boundary. Parameter values are aL=1000, aTeff=56.53, aTreg=198.2, dL=0.01, dTeff=0.2, dTreg=0.04, k1=40, k2=160, k3=200, and p=4.

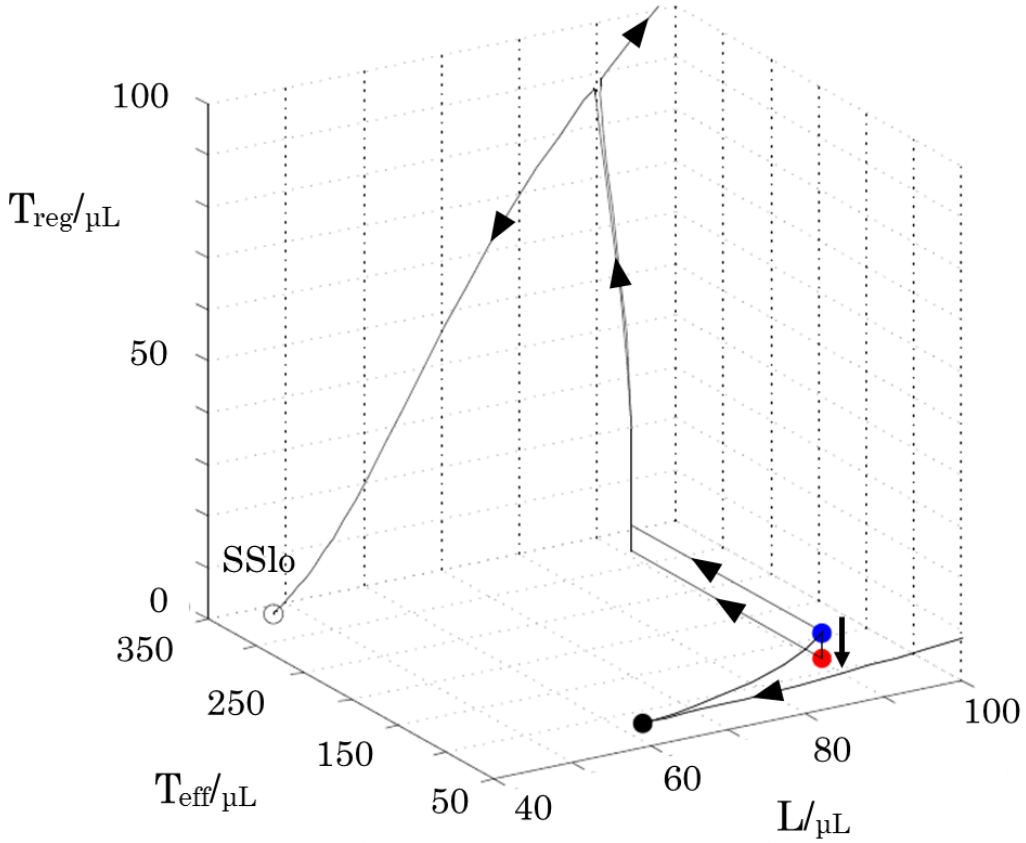

Fig. 6: Effects of Teff infusion only and prior Treg depletion followed by Teff infusion for the system on the trajectory returning to SShi in hypothetical immunotherapy. The instantaneous modulations ([Teff]+200/μl and [Treg]-5/μl) were applied at the point denoted by the blue circle. The Treg depletion forced the system from the point denoted by the blue circle to one denoted by the red circle. The same Teff infusions applied to the points denoted by blue and red circles result in two trajectories, one of which arrives at SSlo (open circle) and another returns to SShi (out of figure). Parameter values are aL=1000, aTeff=56.53, aTreg=198.2, dL=0.01, dTeff=0.2, dTreg=0.04, k1=40, k2=160, k3=200, and p=4. For a chemotherapy duration of 10 days, the decay rate constants were dL=1.0, dTeff=0.7, and dTreg=5.0.